European Journal of Operational Research 297 (2022) 203–220

Contents lists available at ScienceDirect

European Journal of Operational Research

journal homepage: www.elsevier.com/locate/ejor

Decision Support

Pruning Pareto optimal solutions for multi-objective portfolio asset management

Sanyapong Petchrompo[a,*], Anupong Wannakrairot[b], Ajith Kumar Parlikad[a]

[a] Institute for Manufacturing, Department of Engineering, University of Cambridge, 17 Charles Babbage Road, Cambridge CB3 0FS, United Kingdom
[b] University of Bath, Claverton Down Road, Combe Down, Bath BA2 7AY, United Kingdom

ARTICLE INFO

Article history:
Received 9 September 2020
Accepted 27 April 2021
Available online 6 May 2021

Keywords:
Multiple criteria analysis
Multiple objective programming
Pareto pruning
Data clustering
Asset management

ABSTRACT

Budget allocation problems in portfolio management are inherently multi-objective as they entail different types of assets of which performance metrics are not directly comparable. Existing asset management methods that either consolidate multiple goals to form a single objective (*a priori*) or populate a Pareto optimal set (*a posteriori*) may not be sufficient because a decision maker (DM) may not possess comprehensive knowledge of the problem domain. Moreover, current techniques often present a Pareto optimal set with too many options, making it counter-productive. In order to provide the DM with a diverse yet compact solution set, this paper proposes a three-step approach. In the first step, we employ different approximation functions to capture investment-performance relationships at the asset-type level. These simplified relationships are then used as inputs for the multi-objective optimisation model in the second step. In the final step, Pareto optimal solutions generated by a selected evolutionary algorithm are pruned by a clustering method. To measure the spread of representative solutions over the Pareto front, we present two novel indicators based on average Euclidean distance and cosine similarity between original Pareto solutions and representative solutions. Through numerical examples, we demonstrate that this approach can provide a set of representative solutions that maintain high integrity of the original Pareto front. We also put forward suggestions on choosing appropriate approximation functions, pruning methods, and indicators.

1. Introduction

As organisations deploy more infrastructure and equipment to support their operations, the scope of asset management research has shifted from optimising individual asset performance to managing complex systems of multiple assets. For asset intensive industries such as utility and infrastructure, substantial investment is inevitable to maintain assets at a high performing level due to the profound impact of these systems on different stakeholders, often with different objectives. Asset managers are therefore faced with an exacting task in making budget allocation decisions, especially for multi-asset systems that involve multiple objectives.

In a recent study, Petchrompo and Parlikad (2019) categorised a multi-asset system into a fleet and a portfolio. The former is used to describe a group of homogeneous assets or assets that share similar features, whereas the latter is referred to a group of heterogeneous assets. A major factor that complicates the modelling and optimisation of these systems is the fact that multiple units are contingent on each other (Nicolai & Dekker, 2008). To systematise research in the field, existing literature reviews (Olde Keizer, Flapper, & Teunter, 2017; Petchrompo & Parlikad, 2019) usually classified systems based on the interaction among assets/components. Performance dependence occurs when the system performance (e.g. system reliability, safety, and production output) depends on configurations among units (e.g. series, parallel, and *k*-out-of-*N*). Resource dependence exists in a system in which common resources (e.g. budget, equipment, and workforce) are shared among units.

The majority of past portfolio management studies readily assumed inter-asset performance independence and employed simple forms of performance evaluation methods such as sum, average, and percentage to aggregate individual asset performance data into system outputs (Bai, Ahmed, Li, & Labi, 2015; Fwa & Farhan, 2012). Although it is reasonable to make such assumptions for a system that adopts direct physical measures such as asset condition indices, the assumption may not hold for a portfolio that consists of several asset types and requires different performance metrics. For example, infrastructure systems in a manufacturing

* Corresponding author.
E-mail addresses: sp869@cam.ac.uk (S. Petchrompo), anupong@wannakrairot.com (A. Wannakrairot), aknp2@cam.ac.uk (A.K. Parlikad).

https://doi.org/10.1016/j.ejor.2021.04.053

plant or an oil refinery may entail objectives like production output or reliability, which depend on asset configurations (Petchrompo, Li, Erguido, Riches, & Parlikad, 2020; Rasmekomen & Parlikad, 2013). However, to the best of our knowledge, no studies have incorporated inter-asset performance dependence in portfolio management problems due to the formulation complexity.

Budget allocation is one of the most prevalent problem classes in the portfolio management literature (Fwa & Farhan, 2012; Ustun & Anagun, 2015). Although assets in a portfolio may be associated with different intervention options and performance metrics, they are all under the control of a single entity and therefore compete for central budget. Previous papers generally converted and combined multiple criteria into a single criterion before the optimisation process takes place (France-Mensah, O'Brien, & Khwaja, 2019; Sacco, Compare, Zio, & Sansavini, 2019). These methods have proved to be effective in the system involving only a small number of objectives that can be aggregable with other objectives. However, these weighting and combining techniques may not applicable to a problem that involves perspectives from multiple stakeholders or entails multi-type assets with strictly incommensurable performance metrics. To deal with this problem, an alternative strategy is to generate a complete set of non-dominated solutions and visualise these solutions on a trade-off frontier (Bai et al., 2015; Gong & Zhou, 2018). Nonetheless, this method is likely to result in a large number of optimal solutions in high-dimensional space, making it difficult for a DM to comprehend and make a well-informed decision.

In this paper, we consider a budget allocation problem in an asset portfolio with inter-asset performance dependence. In other words, the derivation of a performance objective for an asset type depends on collective outputs from multiple assets (e.g. system reliability is based on a series asset configuration). To overcome the limitations in the existing portfolio management approaches, we propose using a pruning method to address this problem to strike a balance between a single optimal solution and a complete set of non-dominated solutions. The ultimate objective of this approach is to acquaint the DM with the solution space by providing him/her with a subset of representative solutions. The subset of a given size is selected in such a way that strongly represents the original set of non-dominated solutions by maximising the solution diversity.

The remainder of this paper is organised as follows. Section 2 gives a generic problem description and discusses existing work related to the problem of our interest. The overall modelling approach is described in Section 3. Section 4 then introduces the curve-fitting techniques used to approximate investment-performance relationships at the asset-type level. The portfolio optimisation model formulation is presented in Section 5, followed by the discussion on pruning methods in Section 6. In Section 7, three numerical experiments in different problem dimensions are conducted, and the results are discussed. Finally, conclusions and recommendations for future research are given in Section 8.

2. Portfolio budget allocation problem

2.1. Problem description

For a single decision horizon, a DM is required to make investment decisions for maintenance intervention across an asset portfolio. More specifically, the DM has to decide how much budget should be allocated to maintain assets in each asset type in order maximise portfolio performance. The portfolio is comprised of S asset types, each consisting of a fixed number of assets. Each asset type has its own performance measure that is not necessarily comparable to those of other types. This means that the portfolio could possess up to S performance measures, which constitute up to S objectives for the optimisation model. Each of S objective values is derived from the collective performance of multiple assets. Maintenance intervention planning decisions — how and when each individual asset is maintained or enhanced at a specific cost — are determined by an asset-type optimisation model, whereas budget allocation decisions are made at the portfolio level. Specific assumptions associated with the problem are as follows:

- The relationship between the budget allocated to each asset type and its corresponding performance output is assumed deterministic.
- Performance dependence only exists among assets within an asset type.
- Budget is the only form of resource dependence that exists across different asset types.

It is apparent that these assumptions can be met by general portfolio management problems with different asset types, as heterogeneous assets are unlikely to work collectively to generate outputs. A typical example of the problem of interest can be found in the infrastructure network in which each asset type has its own function and the performance thereof can be determined independently of other types. However, these assumptions may not be satisfied in a problem with more complex types of dependence such as inter-type performance dependence (e.g. multi-modal transport network maintenance planning) and workforce and equipment dependence (e.g. maintenance workshop scheduling).

To support decision-making, a reduced set of Pareto optimal solutions is required, so that the results are readily understandable to the DM. Moreover, to provide the DM with comprehensive knowledge of the solution domain, solutions in the reduced set should spread widely across the original Pareto front. Hence, the proposed approach should be able to:

- Aggregate outputs from asset-type models and produce Pareto optimal solutions of all performance metrics across the portfolio.
- Reduce the number of Pareto optimal solutions in a manner that maintains the relative diversity of the reduced set to the original set.
- Perform the aforementioned tasks independently of DM preferences.

2.2. Related work

This section reviews previous research in the portfolio budget allocation problem and discusses potential optimisation methods to issue guidelines on the modelling approach in the next section.

Portfolio budget allocation problems are inherently multi-objective, because they involve different value metrics that are not directly comparable. The approaches adopted by asset management researchers to deal with multiple objectives can be categorised into *a priori* and *a posteriori* modes. The *a priori* mode assumes that all user preferences are known and can be perfectly quantified at the beginning of the decision-making process (Hartikainen, Miettinen, & Klamroth, 2019). In this mode, a DM assigns a weight to each objective, aggregates multiple objectives into a single function, and searches for a single optimal solution. These *a priori* methods generally involve the application of multi-criteria decision analysis (MCDA) in identifying weights and combining multiple objectives (Watrobski, Jankowski, Ziemba, Karczmarczyk, & Ziolo, 2019). On the other hand, in the *a posteriori* mode, a complete set of non-dominated solutions — a Pareto front — is generated by a multi-objective optimisation algorithm (Kellner, Lienland, & Utz, 2019). The DM subsequently makes a trade-off between objectives and selects a preferred solution directly from the Pareto front.

Despite several available *a priori* and *a posteriori* methods, either of the aforementioned methods may not sufficiently address portfolio budget allocation problem. In *a priori* methods, since multiple goals are consolidated to form a single objective, only a single solution is presented to the DM. The aggregation of multiple objectives at an early stage of the resolution process could lead to two problems. First, it is a difficult task for the DM to accurately determine weights for multiple objectives, because only small perturbations in weights can sometimes lead to a dramatic change in the resultant solution. Second, a single solution produced by the optimisation model may not suffice for the DM who wishes to examine different solutions for trade-offs. On the other hand, *a posteriori* methods that populate the entire Pareto optimal set often provide a DM with too many options, making it counter-productive. This problem is apparent in a high-dimensional problem of which the results cannot be effectively visualised and are not easily comprehensible to the DM.

To overcome the weaknesses of these methods, researchers in other fields have developed several approaches for achieving a balance between a single solution and a complete Pareto set. These alternatives will be referred to as *pruning methods* in this paper. In a pruning method, a set of predefined rules is employed to identify a subset of Pareto optimal solutions, so that the solutions are more comprehensible to the DM (Taboada & Coit, 2008). Pruning methods have been applied to system design (Taboada, Baheranwala, Coit, & Wattanapongsakorn, 2007), production planning (Guo, Wong, Li, & Ren, 2013), and workforce allocation (Brusco, 2017). Pruning instructions can be given before, during, or after the optimisation process. In this paper, we broadly classify pruning methods into three classes according to their selection criteria:

- *Preference-based methods:* In this class, pruning instructions are derived from a DM's preference. Typical methods in this class include the non-numerical objective ranking (NOR) and reference-point-based (RPB) methods. In the NOR method, random weights for different objectives are generated in line with the DM's preference before a weighted-sum model is solved for an optimal solution. The process is repeated until a desired Pareto front is complete (Kulturel-Konak, Coit, & Baheranwala, 2008). On the other hand, the RPB method requires the DM to supply a reference point to guide the search towards the region that is of his/her interest. A representative example of RPB method is the PR-MOEA/D developed by Sudeng and Wattanapongsakorn (2015).
- *Efficiency-based methods:* Methods in this class focus on identifying efficient solutions according to pre-set indicators. A typical method in the class is the identification of frontier knees — regions in which a small improvement in one objective could dramatically deteriorate at least one other objective (Sudeng & Wattanapongsakorn, 2016). Another interesting method in this class is the application of data envelopment analysis (DEA). In the study by Li, Liao, and Coit (2009), each of the Pareto optimal solutions generated by an optimisation algorithm is treated as a decision-making unit (DMU). The output of DEA is the relative efficiency of each DMU, which enables the user to identify the most efficient solutions on the Pareto front.
- *Diversity-based methods:* Methods in this class aim at identifying a diverse solution subset in order to provide a DM with comprehensive knowledge of the solution domain. The simplest method in this class is the direct selection of solutions from the Pareto front (Wang, Lin, Fu, Luo, & Chen, 2020b) where the data visualisation is possible. Operational researchers also employed clustering methods to group similar solutions together according to objective values. In clustering methods, a representative solution is selected from each cluster. The DM then investigates the cluster of his/her interest. This technique was introduced to Pareto pruning by Taboada and Coit (2007). Other similar studies include (Cao, Hou, & Gao, 2018; Zio & Bazzo, 2011).

Despite several available techniques, there has not been any definitive indicator that can demonstrate the superiority of a pruning method over another (Sudeng & Wattanapongsakorn, 2015). Hence, the challenge of applying pruning methods lies in the selection of appropriate performance indicators.

3. Modelling approach

As shown in Fig. 1, the proposed approach is comprised of three main steps. Firstly, we determine the relationship between maintenance investment and performance for each of the asset types. The approximation functions derived from the first step are then employed as inputs for a portfolio optimisation model in the second step. The aim of the second step is to make budget allocation decisions across the asset portfolio and generate a Pareto front that demonstrates the trade-offs between the performance objectives. The final step is to identify representative solutions from the Pareto front obtained from the multi-objective optimisation model in the second step. A clustering method is used to partition the solutions into different clusters in such a way that solutions within the same clusters have similar objective values. The selected Pareto subset will consist of central solutions from different clusters in order to preserve the diversity of the original Pareto front. The scope of our approach is defined by dashed boxes in Fig. 1. The approach is started with the modelling of asset-type investment-performance relationship and completed after the representative solution set is obtained.

According to the limitations indicated earlier, the originality of this research paper lies in the following aspects:

- *An approach to approximate input functions for portfolio optimisation:* We propose using different approximation functions to determine investment-performance relationships in the first step. These outputs enable users to simplify an objective function for the optimisation stage while capturing inter-asset performance dependence within an asset type.
- *A framework for pruning Pareto optimal solutions in portfolio management:* To the best of our knowledge, this is the first paper to adopt a pruning method to achieve the balance between *a priori* and *a posteriori* modes to address a portfolio management problem. We also conduct a comparative analysis of the *K*-means and *K*-medoids methods with regards to their application in pruning Pareto optimal solutions.
- *Performance indicators for assessing representative solutions:* With an ultimate goal to provide the DM with a small yet diverse solutions, we develop two performance indicators, Relative Euclidean Index (*REI*) and Relative Cosine Index (*RCI*), for assessing the relative diversity of representative solutions to the original Pareto front.

Despite this paper' s specific application to portfolio management, it is important to note that these techniques can also be applied to any multi-objective problem that follows the assumptions given in Section 2.1.

4. Approximation of investment-performance relationships

This section explains how a continuous function that describes the relationship between the maintenance investment and performance of each asset type can be determined. Existing asset-type models in the literature generally generate a set of non-dominated solutions on a discrete frontier, which demonstrates a trade-off between maintenance investment and collective performance of assets. Fig. 2 depicts two trade-off frontiers, which indicate how

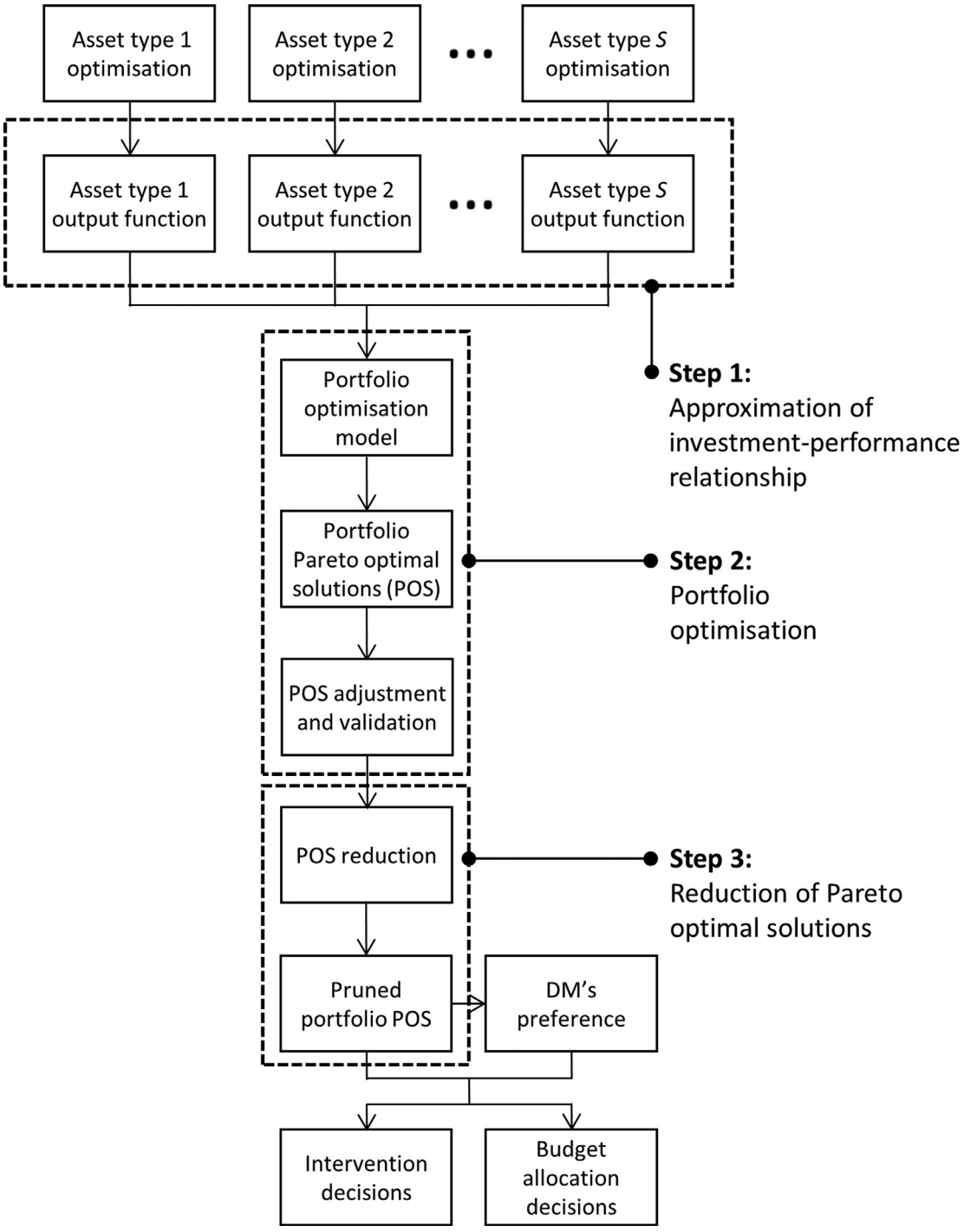

Fig. 1. Structure of the proposed three-step approach.

the asset-type performance (y-axis) is improved as the investment amount (x-axis) increases. Fig. 2a demonstrates how the average remaining useful life of road safety assets increases as more maintenance budget is allocated (Bai et al., 2015). Likewise, Fig. 2b illustrates how the reliability of a power generator system is enhanced as more investment in preventive maintenance is made (Zhong, Pantelous, Beer, & Zhou, 2018).

This investment-performance trade-off information will be used as inputs for the portfolio budget allocation model in the second step. Based on our observations of such relationships in the previous literature (Bai et al., 2015; Fwa & Farhan, 2012; Moghaddam, 2013; Zhong et al., 2018), the trade-off frontiers are generally in the form of discrete data points that illustrate the monotonic relationships between the two value elements albeit having different variants of shapes as shown in Fig. 2. A possible means to feed this information into the portfolio model is to use a binary decision variable to indicate whether an investment-performance pair is chosen at the portfolio level. However, it is apparent that these trade-off frontiers generally consist of many solutions. Therefore, this approach can be very computationally expensive (Koumousis & Katsaras, 2006; Sahoo, Bhunia, & Kapur, 2012). To simplify the input data, we propose employing curve-

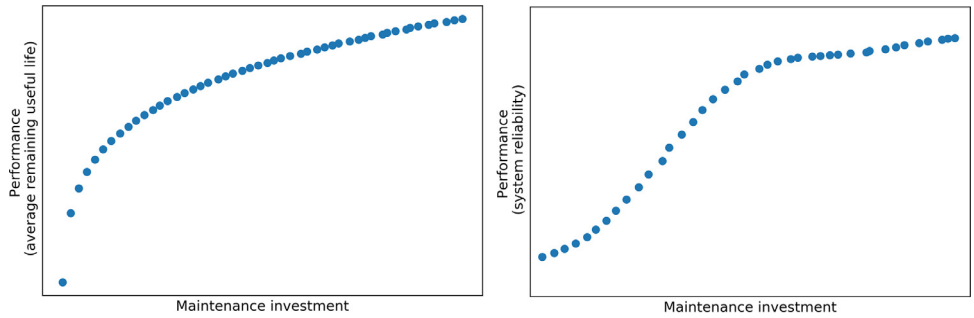

(a) Data adapted from Bai et al. (2015) (b) Data adapted from Zhong et al. (2018)

Fig. 2. Trade-off data representing investment-performance relationships at the asset-type level.

fitting techniques to identify a continuous function that can accurately represent the investment-performance relationship.

Different curve-fitting functions including polynomial (Yang, Gao, Sellars, & Sorooshian, 2015), log-transformed power (Chattopadhyay, Verma, Satsangi, & Sharma, 2009), piecewise linear (Habermann & Kindermann, 2007), spline (De Santiago-Perez, Osornio-Rios, Romero-Troncoso, & Morales-Velazquez, 2013), and radial basis functions (Gneiting, 2013) have demonstrated to produce satisfactory results for approximating different monotonic functions. In spite of several available curve-fitting techniques in the literature, we limit our discussion only to polynomial, log-transformed power, and Gaussian radial basis functions (RBF). Piecewise and spline functions are not included in our discussion because they tend to incorporate a large number of discontinuous sub-functions of which conditional properties could incur high computational cost at the optimisation stage.

It is evident from the previous literature that polynomial fitting is the most popular method because the parameters thereof can be efficiently estimated using the least squares approach. However, polynomial fitting also has some disadvantages in that it is likely to contain a large number of functions with high-degree polynomials in order to achieve an accurate approximate function. On the other hand, log-transformed power functions have been used widely to deal with skewed data and data sets with a power trend.

RBF has been used widely in identifying functions for noisy training data, especially in deep neural network. One major application of RBF is in forecasting. For example, RBF neural networks were used for clustering and regression tasks in a prediction model to forecast the power produced by different variable energy sources (Sideratos & Hatziargyriou, 2020). Moreover, RBF has also been proved to produce high quality approximate functions in different fields. For instance, in robotics, Gaussian RBFs were employed to generate smooth joint trajectories for robot manipulators (Chettibi, 2019). These findings demonstrated that RBF is suitable for approximating scattered data that tend to form a curvilinear shape such as sigmoid or saturation functions. This is due to its accuracy, flexibility, and insensitivity to outliers.

Note that the choice of an appropriate curve-fitting technique and approximation function depends on data characteristics; thus, there is no definitive instruction on which particular curve-fitting method is superior than others. This paper demonstrates the use of log-transformed power functions, polynomial functions, and Gaussian RBFs to approximate investment-performance relationships at the asset-type level. To offer guidelines on choosing an appropriate approximation function, we employ the Nash–Sutcliffe Efficiency coefficient (*NSE*) (Nash & Sutcliffe, 1970) as a goodness-of-fit indicator. *NSE* is expressed as:

$$NSE = 1 - \left(\frac{RMSE}{SD}\right)^2 \tag{1}$$

where *SD* is the standard deviation of the observations and *RMSE* is the root-mean-square error between the actual and estimate data. *RMSE* is given by:

$$RMSE = \sqrt{\frac{\sum_{j=1}^{J}(y_j - \hat{y}_j)^2}{J}} \tag{2}$$

where y_j and $\hat{y}_j$ are the actual data (actual performance data) and the estimate data for observation j of the sample of size J.

Although the *RMSE* can be used to quantify the approximation error, the indicator's wide range (0 to ∞) makes it difficult for a DM to evaluate the goodness-of-fit of a model. By normalising the mean-square error using the variance of the observations, *NSE* is more interpretable. Although *NSE* takes values between $-\infty$ to 1, the indicator generally varies within a finite range. An *NSE* value close to 1 indicates a good fit, whilst a negative *NSE* value suggests that the mean of the observations outperforms the selected approximation function. The detailed guidelines on identifying approximate functions and parameters will be given after the numerical experiments are conducted in Section 7. The remainder of this section introduces the candidate approximation functions.

4.1. Log-transformed power function

The functional relationship between the dependent variable (performance) and the independent variable (maintenance investment) with a power trend can be expressed as:

$$y = ax^b \tag{3}$$

where y is the dependent performance variable and x is the independent variable; a and b are parameters.

Eq. (3) can be converted into a linear form by logarithmic transformation and rewritten as:

$$\log(y) = \log(a) + b\log(x) \tag{4}$$

Eq. (4) can also be written as:

$$\tilde{y} = \alpha_0 + \alpha_1 \tilde{x} \tag{5}$$

where $\tilde{y}$ is the value of the dependent performance variable on a logarithmic scale and $\tilde{x}$ is the logarithmic transformation of the investment variable; α_0 and α_1 are the intercept and regression coefficient respectively. The linear regression model is fitted using the least squares approach.

4.2. Polynomial function

The polynomial function of degree M is given by:

$$y = \beta_0 + \beta_1 x + \beta_2 x^2 + \cdots + \beta_M x^M \tag{6}$$

where $\beta_0, \beta_1, \beta_2, \ldots, \beta_M$ are the coefficients of the polynomial. For the parameter estimation purpose, the polynomial function can be

considered linear where $x, x^2, \ldots, x^M$ are independent variables. As with the log-transformed model, the polynomial regression model can be fitted using the least squares approach.

4.3. Gaussian radial basis function

A radial basis function is a real-valued function whose value depends on the distances between the input variable and selected fixed points. Using Gaussian as a basis function, the Gaussian RBF with M functions can be defined as:

$$y = \sum_{i=1}^{M} w_i e^{-\varepsilon_i (x-p_i)^2} \tag{7}$$

where y is the dependent performance variable and x is the investment variable; w_i, ε_i, and p_i are the coefficient, shape parameter, and centre of Gaussian function i respectively.

Since there is no closed form solution for obtaining Gaussian RBF parameters, it is necessary to employ an algorithm that can train the data in such a way that the loss function — the sum of the differences between estimate and actual empirical values of data — is minimised. Recent studies used a variety of algorithms including genetic algorithms, grid search, and gradient descent techniques to determine these parameters (Ma, Liu, & Cao, 2019; Serfidan, Uzman, & Turkay, 2020). In this research, we employ a gradient descent optimisation algorithm called *adaptive data momentum* (Adam) optimisation to estimate parameters ε_i and p_i. Adam is an extension of gradient descent optimiser, based on adaptive estimates of lower-order moments. Adam is chosen over other stochastic gradient descent methods due to its learning speed, low computation complexity, and little memory requirements (Kingma & Ba, 2014). More importantly, the method is straightforward to implement as its hyperparameters have intuitive interpretations. After ε_i and p_i are obtained, Eq. (7) can be rearranged in a linear form where $e^{-\varepsilon_i (x-p_i)^2}$ is the regressor. Thus, the coefficient w_i can be obtained using the least squares approach. The details of the algorithm can be found in the pseudocode given in Appendix A. During the training process, we calculate the gradient of the loss function with respect to the hyperparameters. Employing the same expressions for y_j and $\hat{y}_j$ as given in Eq. (2), we can define the loss function L using the sum of squared errors (SSE):

$$L = \sum_{j=1}^{J} (y_j - \hat{y}_j)^2 \tag{8}$$

Since the goal of applying Gaussian RBF is not to predict but to interpolate a function for the data within a selected dataset, the problem of data overfitting will not arise. Hence, all of the solutions on the investment-performance frontier will be used in the training process.

5. Portfolio optimisation

After the relationship between the maintenance investment and performance of each asset type is determined, the next step is to decide how much budget should be allocated to each asset type to optimise portfolio performance. This section explains the portfolio optimisation model employed in the second step of the proposed approach. Apart from the model formulation, we also discuss the multi-objective optimisation algorithms and solution validation approach adopted in this paper.

5.1. Multi-objective optimisation model formulation

Based on the problem description given in Section 2, the optimisation model for a portfolio of S asset types can be formulated as:

$$\max g_i(x_i) \text{ for } i = 1, 2, \ldots, S \tag{9}$$

subject to:

$$\sum_{j=1}^{S} x_i \le B \tag{10}$$

$$c_i^{\min} \le g_i(x_i) \le c_i^{\max} \text{ for } i = 1, 2, \ldots, S \tag{11}$$

where x_i is the decision variable determining the amount of budget allocated to asset type i; $g_i(x_i)$ is the performance measure i as a function of x_i; B is the total budget for asset management planning in the considered decision horizon; $c_i^{\min}$ and $c_i^{\max}$ are the minimum and maximum performance levels allowed for the performance measure i respectively.

Objective function (9) is set to maximise performance of multiple asset types. Each of the functions $g_i(x_i)$ is derived from Step 1. Constraint (10) indicates that the sum of investments in all asset types cannot exceed the total budget, while Constraint (11) specifies the feasible range of performance levels for each asset type.

5.2. Optimisation solution methods

We first populate a complete set of non-dominated solutions before they are pruned in the next step. The concept of non-dominance — the Pareto optimality — can be explained using the following example.

Let $\mathbf{a} = [a_1, a_2, \ldots, a_K]$ and $\mathbf{b} = [b_1, b_2, \ldots, b_K]$ be two different vectors of K decision variables and $I = \{1, 2, \ldots, S\}$ be a set of S objectives. In a multi-objective maximisation problem, the vector $\mathbf{a}$ dominates vector $\mathbf{b}$ if and only if:

$$g_i(\mathbf{a}) \ge g_i(\mathbf{b}) \text{ for all } i \in I \text{ and } g_i(\mathbf{a}) > g_i(\mathbf{b}) \text{ for at least one } i \in I \tag{12}$$

where $g_i(\mathbf{x})$ is the value of objective i as a function of decision variable $\mathbf{x}$.

A solution is considered Pareto optimal if the value of one objective cannot be improved without negatively affecting at least one of the other objectives (Raimundo, Ferreira, & Von Zuben, 2020). To work towards a comprehensive set of Pareto optimal solutions, previous researchers made great strides in developing multi-objective evolutionary algorithms (MOEAs). The existing MOEAs can be categorised by their methods to balance the convergence and diversity of solutions on the approximated Pareto front, namely into Pareto dominance based and decomposition based (Hafiz, Swain, & Mendes, 2020). A representative algorithm from each of the two categories — Non-dominated Sorting Genetic Algorithm-II (NSGA-II) (Deb, Agrawal, Pratap, & Meyarivan, 2000) and Multi-objective Evolutionary Algorithm based on Decomposition (MOEA/D) (Zhang & Li, 2007) — is employed. Since the development of MOEAs is not a major contribution of this paper, we only demonstrate that the selected algorithms can produce effective solutions based on a selected indicator.

5.2.1. NSGA-II

In NSGA-II (Deb et al., 2000), solutions are ranked using a fast non-dominated sorting approach. The process begins with a set of non-dominated individuals identified and assigned rank 0. Next, the second set of non-dominated individuals is generated and assigned rank 1. The process continues until the entire population is examined. Individuals of lower ranks have the priority to survive. In case the number of solutions of the same rank is larger than the archive size, the crowding distance mechanism is applied to preserve the solution diversity. Specifically, among candidate solutions of the same rank, less crowded individuals will be selected

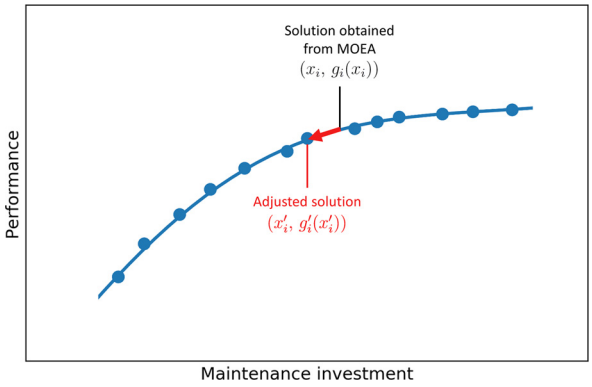

Fig. 3. Solution adjustment operation from a single-objective perspective.

to enter the archive. By sorting the population based on each objective value and assigning a large distance value to extreme solutions, the algorithm is likely to select extreme solutions in the next population. The elitism of the solutions is ensured by retaining all the non-dominated solutions throughout the generations.

5.2.2. MOEA/D

In MOEA/D (Zhang & Li, 2007), a multi-objective optimisation problem is explicitly decomposed into multiple scalar optimisation sub-problems. The decomposition is facilitated by a scalarising function and a set of uniformly distributed weight vectors. Specifically, each sub-problem is assigned with a specific weight vector. The fitness value of a solution vector for each sub-problem is then computed by a scalarising function. The Tchebycheff function is used as a decomposition function in this paper. The decomposition process enables MOEA/D to effectively address fitness assignment and diversity maintenance issues, which are problematic in traditional decomposition MOEAs. Moreover, by employing a small population to produce a small number of evenly distributed solutions, MOEA/D tends to incur low computational cost at each generation when compared to other MOEAs. Note that, in MOEA/D, the population size corresponds to the number of generated weight vectors because only one best solution is stored for each sub-problem.

5.3. Solution adjustment and validation

The outputs obtained from the multi-objective optimisation model defined in Section 5.1 are based on the investment-performance functions derived in Section 4. This means that these outputs may not perfectly correspond to original asset-type outputs and could fall into infeasible space. To ensure that the final solutions obtained from the portfolio optimisation model are feasible, an adjustment to these outputs is necessary. The pseudocode for the adjustment operation is given in Appendix B. The adjustment operation from a single-objective perspective is illustrated in Fig. 3. Suppose that for objective i, the value $g_i(x_i)$ is a Pareto optimal value generated by an MOEA. Since the coordinate x_i, $g_i(x_i)$ may not correspond to any actual asset-type solution, the algorithm will identify x'_i and $g'_i(x'_i)$. The former is the largest feasible x value that does not exceed x_i, while the latter is the corresponding feasible objective value. By doing so in every dimension, an adjusted Pareto optimal set can be obtained.

Nonetheless, after the adjustment, some solutions may duplicate their adjacent solutions or become inferior to other adjusted solutions. To remove redundant and dominated outputs, a Pareto optimality check on the adjusted solutions is conducted. The solution validation process complies with the condition set out in Statement (12). Once all the inferior and duplicate solutions are removed, the validated Pareto optimal set can be attained.

5.4. Solution performance indicator

To evaluate the performance of our optimisation method and compare the quality of MOEAs, the hypervolume metric is adopted. In its application to multi-objective optimisation, hypervolume is defined as the objective space enclosed by a reference point and a set of solutions generated by a selected algorithm (Zitzler & Thiele, 1999). Based on its straightforward calculation, hypervolume has an ability to measure both the solution convergence and diversity, thereby meeting the requirements set out in our problem description. The hypervolume indicator has been employed to determine and compare performance of MOEAs in recent studies on multi-objective optimisation (Raimundo et al., 2020; Wang, Li, Tao, & Gu, 2020a).

For the purpose of hypervolume calculation in a maximisation problem, each objective function value i is linearly normalised as:

$$g''_i(x'_i) = \frac{g'_i(x'_i) - g_i^{\min}(x'_i)}{g_i^{\max}(x'_i) - g_i^{\min}(x'_i)} \text{ for } i = 1, 2, \ldots, S \tag{13}$$

where $g''_i(x'_i)$ is the value of normalised objective function i; $g'_i(x'_i)$ is the adjusted and validated value of objective i; $g_i^{\min}(x'_i)$ and $g_i^{\max}(x'_i)$ are minimum and maximum values of objective function i found in the feasible solution space respectively.

A reference point is required to determine the hypervolume indicator of a given non-dominated front. In this paper, we take up the suggestion offered by Araya, Moyano, and Sanchez (2020); Ishibuchi, Imada, Setoguchi, and Nojima (2018) on how to select an appropriate reference point. By its definition, the reference point must be dominated by all the efficient solutions. Given the nadir point N and ideal point I, the reference point R can be given by:

$$R = N - r(I - N) \tag{14}$$

Ishibuchi et al. (2018) propose to use r close to $1/u$ where u is the number of solutions on the Pareto front.

6. Reduction of Pareto optimal solutions

In the final step of our proposed approach, the Pareto optimal solutions obtained from the portfolio optimisation model are pruned before they are delivered to the DM. The goal of pruning is to provide a compact yet diverse solution set that is easily comprehensible to the DM. A comparison of Pareto pruning methods discussed in Section 2.2 against the problem requirements is drawn in Table 1.

It is apparent that the preference-based method is reliant on the DM' s preferences, whereas the efficiency-based method only considers the relative efficiency of the solutions, thereby neglecting the diversity criteria. This means that the diversity-based method is the only pruning method that satisfies all the requirements because the selection of representative solutions is based on solution coordinates. Hence, the remainder of this paper will focus on clustering — the most widely used diversity-based pruning method.

Clustering is a type of unsupervised learning methods in which data points are divided into clusters. The data is clustered in such a way that data points in the same cluster are more similar and data points across different clusters are more dissimilar. Although various clustering techniques are available in the previous literature, our discussion is limited to two methods: K-means and K-medoids. The K-means method is chosen as a benchmark because it is the most popular clustering method used in the existing literature on Pareto pruning. The K-medoids is chosen as a candidiate because it uses an actual data point (medoid) as a cluster centre. This characteristic allows the user to identify representative solutions without any adjustment.

Table 1
Comparison of pruning methods against the problem requirements.

Requirement	Pruning methods		
	Preference-based	Efficiency-based	Diversity-based
Solution reduction	✓	✓	✓
Independence of DM's preferences		✓	✓
Diversity preservation			✓

6.1. K-means clustering

The *K*-means method was pioneered by MacQueen (1967). The *K*-means method is renowned for its efficiency and straightforward interpretation. The essence of the*K*-means method is the assignment of data points to clusters and the computation of cluster centres (centroids) according to the Euclidean distance. The method seeks to organise N data points from a set of observations $\mathbf{v} = \mathbf{v}_1, \mathbf{v}_2, \ldots, \mathbf{v}_N$ into K clusters $\mathbf{C} = C_1, C_2, \ldots, C_K$ with an objective to minimise the sum of squared deviation of data points to their corresponding centroids. The objective of the *K*-means method is to find:

$$\arg\min_{\mathbf{C}} \sum_{j=1}^{K} \sum_{\mathbf{v}\in C_j} \left\| \mathbf{v} - \mathbf{d}_j \right\| \tag{15}$$

where $\mathbf{d}_j$ is the centroid vector of cluster j; $\|.\|$ denotes the Euclidean norm.

In its particular application to Pareto pruning, the *K*-means method requires an additional step in identifying cluster representatives. Since a centroid is the mean of solutions in a cluster, the *K*-means method cannot guarantee that the centroid is a member of the original dataset. To choose an appropriate cluster representative, previous researchers suggested using the closest solution (according to Euclidean distance) to each centroid (Taboada & Coit, 2007).

6.2. K-medoids clustering

The *K*-medoids or partitioning around medoids method was proposed by Kaufmann and Rousseeuw (1987). The *K*-medoids method also aims at minimising the distance (maximising similarity) between data points and a designated cluster centre. However, the difference lies in the identification of cluster centre. While *K*-means uses calculated means as cluster centres, the *K*-medoids method uses actual data points (medoids) as cluster centres. Hence, the use of medoids offers more flexibility as it allows the use of any distance or similarity metric for clustering. In this paper, the cosine similarity is adopted; Using the same expressions for $\mathbf{C}$ and $\mathbf{v}$, the objective of the *K*-medoids method can be given by:

$$\arg\max_{\mathbf{C}} \sum_{j=1}^{K} \sum_{\mathbf{v}\in C_j} \frac{\mathbf{v}\cdot\mathbf{m}_j}{\|\mathbf{v}\|\left\|\mathbf{m}_j\right\|} \tag{16}$$

where $\mathbf{m}_j$ is the medoid vector of cluster j.

6.3. Performance indicators for representative solutions

Difficulties inherent in applying clustering techniques lie in the determination of the appropriate number of clusters and the comparison of different clustering methods. Various clustering indicators have been proposed in the previous literature. Taboada and Coit (2007) suggested the use of silhouette index which compares the intra-cluster to the inter-cluster data similarity based on the average Euclidean distance. In a more recent study, Brusco (2017) proposed using a ratio indicator that determines the improvement in a measure objective when K increases (comparing the improvement of increasing from $K-1$ to K with that of K to $K+1$).

Although the silhouette index can evaluate the quality of clustering based on how distant an individual data point is from neighbouring observations, it does not indicate how well a selected centre represents other solutions within its cluster. Thus, the silhouette index does not comply with the problem requirement for the assessment of the reduced set to the original Pareto set. Objective improvement indicators also have several limitations. Firstly, a measure of a method may not be applicable to other methods. Secondly, for some specific measures such as sum of squared Euclidean distance, it is difficult to determine a threshold that distinguishes desired from undesired results.

To transcend the limitations of existing indicators, we develop two new indices: *relative Euclidean index* (*REI*) and *relative cosine index* (*RCI*). Instead of assessing the distance of every single data point from neighbouring observations, the proposed indices compute the distance (or similarity) between any data point and its nearest representative solution. In other words, superior *REI* and *RCI* values suggests that unselected Pareto optimal solutions are not significantly different from one of the representative solutions. Both indices use the normalised solutions $g''(x')$ previously defined in Eq. (13) in their calculation.

To enhance the interpretability of these indicators, the formulation of both indices is based on the worst-case and best-case scenarios as depicted in Fig. 4 where round (○) and plus (+) markers represent original Pareto and representative solutions respectively. The worst-case scenario (Fig. 4a) demonstrates a poor relative diversity of the representative solution as only one single solution is used to reflect the entire Pareto front. Contrarily, the best-case scenario (Fig. 4b) demonstrates the ideal case in which all solutions are captured in the representative subset. The use of these reference scenarios in *REI* and *RCI* will be discussed after are formally defined in the remainder of this section.

6.3.1. Relative euclidean index

The relative Euclidean index can be defined as:

$$REI_K = \frac{\varepsilon_K}{\varepsilon_1} \tag{17}$$

where REI_K is the relative Euclidean index for a representative Pareto set of K solutions. ε_K is the average of the sum of squared Euclidean distances between original solutions and their closest representative solutions.

Given an original Pareto optimal set of N solutions and a representative solution set of K members $\mathbf{p}^K$, the average of sum of squared Euclidean distances between original solutions and their closest solutions in the representative set ε_K is given by:

$$\varepsilon_K = \frac{1}{N}\sum_{i=1}^{N} \min_j \left\| \mathbf{v}_i - \mathbf{p}_j^K \right\| \tag{18}$$

Based on Eqs. (17) and (18), *REI* is a measure of the average distance between representative solutions and all solutions on the Pareto front. The value of *REI* ranges from 0 to ∞. An *REI* value close to 0 suggests that the selected solution set can strongly represent the original Pareto front, thereby implying a high relative

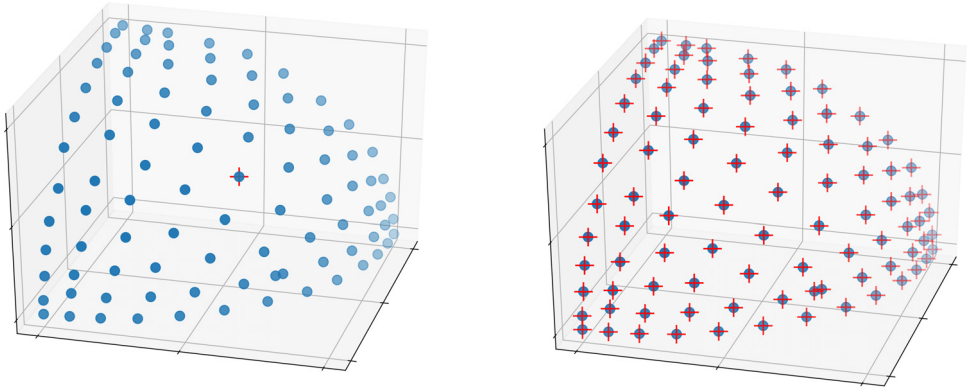

(a) Worst-case scenario (b) Best-case scenario

Fig. 4. Benchmark scenarios for relative diversity indicators.

diversity of the representative solutions. Contrarily, an *REI* value greater than 1 shows that even a single central solution outperforms the selected solution set and therefore suggests that the representative solutions poorly reflects the characteristic of the original Pareto front.

6.3.2. Relative cosine index

The relative cosine index is given by:

$$RCI_K = \frac{\gamma_K - \gamma_1}{1 - \gamma_1} \tag{19}$$

where RCI_K is the relative Euclidean index for a representative Pareto set of K solutions. γ_K is the average of cosine similarities between original solutions and their closest representative solutions.

For a representative set of K solutions $\mathbf{p}^K$, the average of cosine similarities between original solutions and their closest representative solutions γ_K is given by:

$$\gamma_K = \frac{1}{N}\sum_{i=1}^{N} \max_j \frac{\mathbf{v}_i \cdot \mathbf{p}_j^K}{\|\mathbf{v}_i\| \left\|\mathbf{p}_j^K\right\|} \tag{20}$$

As shown in Eqs. (19) and (20), the interpretation of *RCI* differs from that of *REI*. This is due to the use of cosine measure in which a high value demonstrates strong similarity between a pair of observations. The *RCI* value ranges from $-\infty$ to 1, and its interpretation is in the opposite direction to *REI*. A high *RCI* value (close to 1) indicates that the selected centres are similar to other data points in their clusters, thereby signifying a widespread distribution of representative solutions along the original Pareto front. Contrarily, a negative *RCI* value suggests that the representative solution set is worse than a single central solution.

7. Numerical examples

In this section, we employ three different examples to demonstrate the application of the pruning methods and performance indicators described in the previous sections. Example I borrows the outputs obtained from existing studies to demonstrate how our proposed approach can be applied to the investment-performance information obtained from asset-type optimisation models. Example II considers a real-world portfolio management problem in a railway network. This example shows that our approach can utilise the outputs obtained from asset-type simulation models provided by our industrial partner. Lastly, in Example III, the bi-objective DTLZ2 problem is employed to warrant the proposed pruning methods and performance indicators. Note that all the algorithms were coded in Python 3.7 and run on a PC with 2.4GHz Intel®Core™ i5 processor.

7.1. Example I

In this example, we consider a problem in a manufacturing plant in which a DM has to make budget allocation decisions for a portfolio of three asset types. The trade-off frontiers that represent the relationship between maintenance investments and performance metrics for each asset type is borrowed from well-known asset management studies.

Assets in the first type are a group of safety assets (Bai et al., 2015). The average remaining service life (RSL) was used to evaluate the performance of this asset type. In other words, the trade-off frontier represents the relationship between the average RSL and cost of maintenance required to achieve the RSL. The second asset type is a multi-workstation manufacturing system (Moghaddam, 2013) with three possible maintenance actions (repair, replace, and do nothing). The evaluation of the system' s performance (system reliability) is based on a series configuration of multiple workstations. The trade-off frontier represents the relationship between reliability and cost of maintenance. The third asset type is a system of power generators (Zhong et al., 2018). The original asset-type model was developed to optimise preventive maintenance plan with two conflicting objectives: maximising system reliability and minimising maintenance cost. The reliability is derived from a gross power reserve function, which is the difference between the demand and the aggregate amount of electricity produced by all generators.

The combination of the three asset types ($S = 3$) leads to a portfolio management problem with three conflicting objectives: maximising RSL of Asset type 1, maximising reliability of Asset type 2, and maximising reliability of Asset type 3. The manufacturing plant has a budget of 3 million GBP. The summary of the information used in this example is given in Table 2. In this example, the investment spending will be stated in 10^5 GBP.

Table 2 shows that maximum performance can be achieved by spending at the maximum investment level for each asset type. It is apparent that implementing the ideal maintenance plan for each of the asset types will violate the organisation' s budget constraint. Hence, budget allocation decisions need to be optimised across the portfolio.

7.1.1. Approximation of investment-performance relationships

To determine appropriate functions that will be used as inputs to the portfolio optimisation model, the investment-performance data are approximated using the candidate functions described in Section 4. Performance of different approximation functions for the three asset types is illustrated in Fig. 5, which demonstrates how the *NSE* (y-axis) improves as the number of functions (x-axis)

Table 2
Summary of investment-performance information at the asset-type level (Example I).

Asset type	Assets	Objective	Investment range		Performance range	
			min	max	nadir	ideal
1	Safety assets	max average RSL	0.00	20.32	2.9359	12.0793
2	Manufacturing system	max reliability	2.96	35.67	0.0243	0.7311
3	Power generators	max reliability	0.00	28.39	0.6839	0.8449

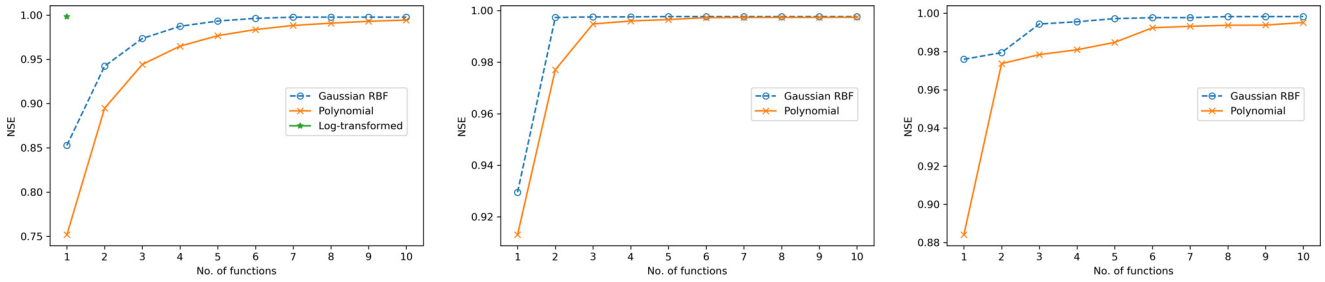

(a) Asset type 1 (b) Asset type 2 (c) Asset type 3

Fig. 5. Performance of approximation functions (Example I).

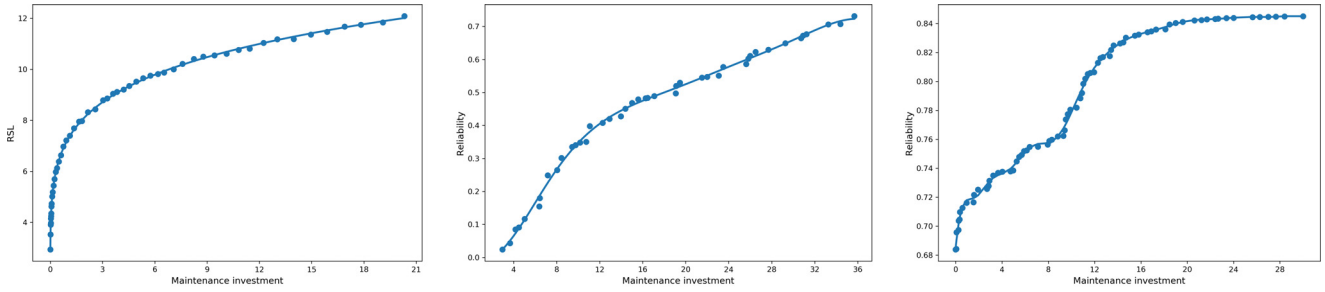

(a) Asset type 1 (b) Asset type 2 (c) Asset type 3

Fig. 6. Curve fitting for investment-performance relationships (Example I).

incorporated in the approximate functions increases. Due to the rigidity and limitation of the log-transformed power function, its outputs are presented only when they are comparable to those of the polynomial and Gaussian RBFs. The investment-performance data for all asset types and the selected smooth curves that represent the relationships thereof are depicted in Fig. 6.

Fig. 5 shows that the improvement in *NSE* stalls when the number of functions reaches a certain point, indicating the convergence of these functions. These findings enable us to identify the appropriate number of functions to be incorporated in the polynomial functions and Gaussian RBFs.

For Asset type 1, Fig. 5a demonstrates that both polynomial and Gaussian RBFs are outperformed by the log-transformed power function even if the first two employ larger numbers of functions. This is because the investment-performance relationship of this asset type appears to have a power trend as shown in Fig. 6a. Hence, the linear regression with logarithmic transformation described in Eqs. (3)–(5) is used to approximate the function for Asset type 1. The least squares approach provides the estimates for the parameters $\alpha_0 = 1.9805$ and $\alpha_1 = 0.1677$ and gives $NSE = 0.9995$. Hence, the power function described in Eq. (3), where $a = 0.7247$ and $b = 0.1677$ will become the first objective function to be maximised in the portfolio optimisation model.

It is evident from Fig. 5b–c that, for both Asset types 2 and 3, the Gaussian RBFs are superior to the polynomial functions as the former produces higher *NSE* values in every scenario. Moreover, the Gaussian RBFs have also shown to converge using fewer numbers of functions (M) than the polynomial functions. Specifically, our experiments have demonstrated that the *NSE* values for Asset types 2 and 3 cease to improve at 0.9977 ($M = 5$) and 0.9983 ($M = 8$) respectively. Thus, we can put forward suggestions to use the Gaussian RBFs as given in Eq. (7) with the parameters exhibited in Appendix C as the second and third objective functions for the portfolio optimisation model in the next step.

7.1.2. Portfolio optimisation

The investment-performance functions derived from Step 1 are used as inputs for the portfolio optimisation model in Step 2. The multi-objective optimisation model is then solved by NSGA-II and MOEA/D. Due to the stochastic nature of both MOEAs, we determine the performance of each algorithm over 30 independent runs. Since the development of MOEAs is not the contribution of this paper, we only employ the parameters that were found to produce satisfactory results in a previous study (Hafiz et al., 2020). It is recommended that related parameters are tuned if these algorithms were applied to an actual industrial use or a study focusing on the development of MOEAs. More information on parameter tuning for NSGA-II and MOEA/D can be found in Samsuri, Ahmad, Zakaria, and Zain (2019), Pang, Ishibuchi, and Shang (2019). In this paper, we employ the crossover and mutation probabilities of 0.9 and 0.006 for NSGA-II and 0.8 and 0.008 for MOEA/D respectively. We use the population size of 600 for both MOEAs and fix the neighbourhood size for MOEA/D at 10% of the population size.

The hypervolume indicator is employed to assess and compare the two MOEAs after the solutions obtained from these algorithms are adjusted and validated. In our experiments, the average num-

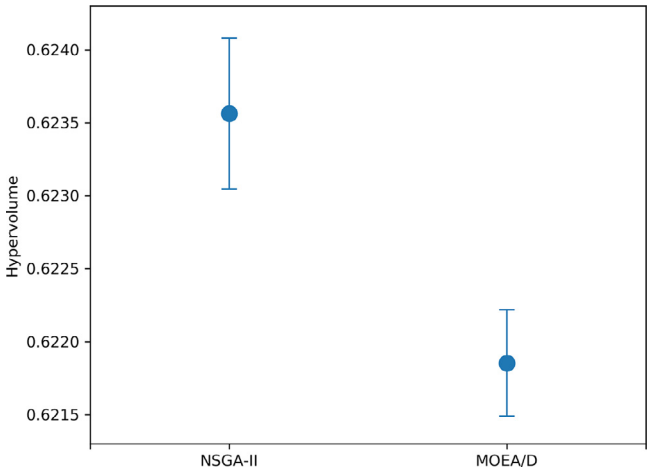

Fig. 7. 95% Confidence intervals for the mean hypervolume (Example I).

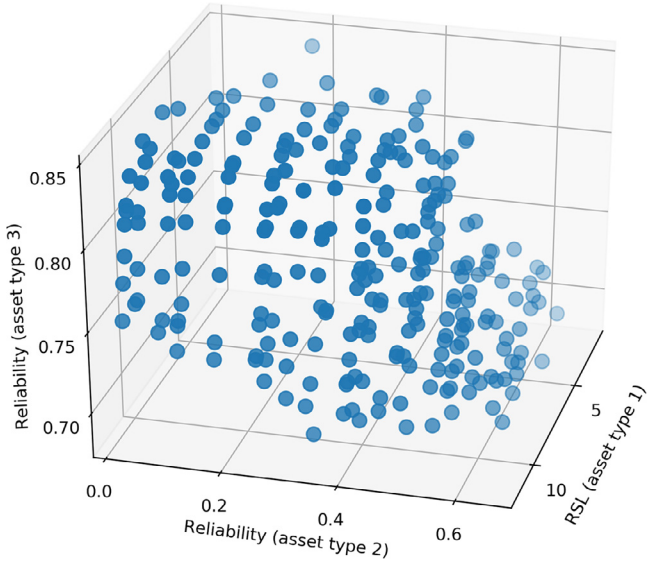

Fig. 8. Pareto front of validated solutions (Example I).

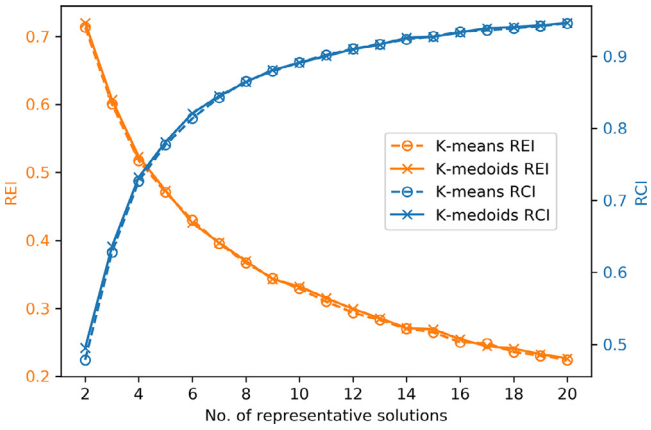

Fig. 9. Relative diversity against the number of representative solutions (Example I).

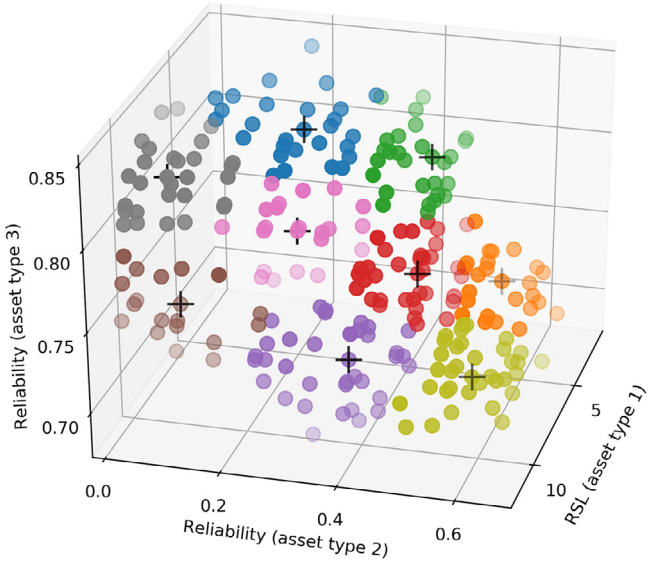

Fig. 10. Representative solutions and solution clusters (Example I).

ber of solutions on the Pareto front obtained from multiple runs of NSGA-II and MOEA/D is 252.25. Hence, we use $r = 1/253$ for calculating the reference point in Eq. (14). The mean hypervolume values and the corresponding 95% confidence intervals produced by the two algorithms are illustrated and compared in Fig. 7. It is visually apparent from the plot that NSGA-II outperforms MOEA/D in this example. The confidence interval for the mean hypervolume derived from 30 runs of NSGA-II is (0.6231, 0.6241), while that of MOEA/D is (0.6215, 0.6222). Further analyses on this example will be based on the results obtained from the best run of NSGA-II which gives the highest hypervolume of 0.6257.

Fig. 8 depicts the non-dominated solutions obtained from NSGA-II after the solution adjustment and validation operations are performed. Although 342 inferior and duplicate solutions have been eliminated, the DM still needs to handle 258 remaining solutions in the validated set. To make these solutions easily comprehensible to the DM, we will demonstrate how pruning methods can be used to reduce the number of solutions in Step 3.

7.1.3. Reduction of Pareto optimal solutions

The *K*-means and *K*-medoids algorithms were applied to clustering 258 solutions from the validated Pareto optimal set. To identify the appropriate number of clusters, we determine the relative diversity of the representative solutions with K varied between 2 and 20. Fig. 9 illustrates the *REI* and *RCI* values of the representative solutions generated by the selected algorithms. The values of ε_1 and γ_1 used in the calculation of *REI* and *RCI* are determined by Eqs. (18) and (20), both at $K = 1$, respectively.

Fig. 9 indicates that the performances delivered by the *K*-means and *K*-medoids methods are closely comparable. The results indicate that, at small K values, both diversity indicators improve significantly as K increases, but the improvement becomes less significant once K reaches a certain level. The analysis can be informative for a DM who seeks to derive benefits from having more solutions in the representative set. A set of nine representative solutions ($K = 9$), which is deemed the elbow point, will be used to demonstrate the next step of the proposed pruning method. Note that this K value is used only for demonstration purposes; in reality, any number of solutions can be chosen according to the perspective of a DM.

The nine clusters produced by the *K*-medoids method are depicted in Fig. 10. In this example, the *K*-medoids was chosen over the *K*-means method because the former resulted in a lower *REI* of 0.3432 and a higher *RCI* of 0.8810. In Fig. 10, solution clusters are differentiated by colours, and the medoid of each cluster is represented by a plus (+) marker. It is visually apparent that the clustering is effective, as members within a cluster are in the same region

Table 3
Summary of investment-performance information at the asset-type level (Example II).

Asset type	Assets	Objective	Investment range		Performance range	
			min	max	nadir	ideal
1	Signalling assets	min SDC	150.00	230.00	223.56	207.23
2	Tracks	min SDC	270.00	356.00	207.31	182.23
3	Earthworks	max RAV	170.00	260.00	2547.76	2581.56
4	Structures	max RAV	200.00	350.00	4187.00	4424.62

of the three-dimensional space with their corresponding medoid located approximately in the cluster centre. It is also noticeable that the medoids are well spread throughout the Pareto front. Supported by the *REI* and *RCI* indicators, our clustering method has proved to maintain high relative diversity of the reduced Pareto set — the ultimate objective of our pruning approach. Representative solutions of the nine clusters (budget allocation decisions and objectives) are summarised in Appendix C. Note that the visualisation as in Fig. 10 can be presented to the DM to bolster the decision-making process. However, this is only possible in two- and three-dimensional problems. For a problem in higher-dimensional space in which the visualisation of solutions is ineffective, a list of representative solutions as in Appendix C is provided instead.

7.2. Example II

Example II is adapted from an exploratory case study on a UK-based rail network. This case study focuses on an intervention planning for a selected route. In this particular route, the asset manager aims to devise a 30-year intervention plan for a portfolio of four asset types ($S = 4$): signalling assets, tracks, earthworks, and structures. The company adopts functional metrics to assess performance of systems that directly affects the service in addition to traditional condition metrics. Note that the numerical figures presented in this example are slightly masked and scaled due to confidentiality issues.

The investment-performance relationship of each asset type is determined by a simulation model developed by the company. The simulation model considers the asset condition that corresponds to an investment level and uses historical system failure data to determine the performance for each asset type. In this example, the expected performance value is used as the input to the proposed model. Since the condition of the assets in the first two types — signalling assets and tracks — directly affects the train performance, the service disruption cost (SDC) is used as the performance metric. On the other hand, the overall remaining asset value (RAV) is used to assess the performance for earthworks and structures.

The company has a budget of 950 million GBP for the four asset types throughout the 30-year time span. This leads to a portfolio optimisation problem with four objectives: minimising SDC for Asset types 1–2 and maximising RAV for Asset types 3–4. The investment-performance information used in Example II is summarised in Table 3. In this example, the investment spending is stated in million GBP.

7.2.1. Approximation of investment-performance relationships

Performance of approximation functions, determined by the *NSE* against the number of functions, is illustrated in Fig. 11. Fig. 11a–b demonstrates that the Gaussian RBFs clearly outperform the polynomial functions when using the same number of functions. Contrarily, Fig.11c–d shows that performance of the Gaussian RBFs and polynomial functions are closely comparable after the *NSE* values of both functions converge. According to these results, we can put forward suggestions to use Gaussian RBFs with $M = 8$ and $M = 9$, which gives the *NSE* values of 0.9996 and 0.9997 for Asset types 1 and 2 respectively. Contrarily, we suggest using polynomial functions with $M = 7$ and $M = 3$, which results in the *NSE* values of 0.9987 and 0.9996 for Asset types 3 and 4 respectively. The polynomial functions, albeit produce comparable results, are chosen over Gaussian RBFs, because the computational cost for estimating function parameters incurred by the least squares approach is lower than that of Algorithm 1 exhibited in Appendix A. The parameters of the Gaussian RBFs and polynomial functions that will be used as objective functions in the optimisation stage are summarised in Appendix D. The smooth curves produced by the chosen approximation functions are depicted in Fig. 12.

7.2.2. Portfolio optimisation

The approximation functions determined in the previous section are used as objective functions in the portfolio optimisation model. This example employs the same parameters as those in Example I, except for the population size of 1000. The reference point is also estimated by Eq. (14) using $r = 1/689$, which is determined from the average number of solutions from 30 runs of both algorithms.

The mean hypervolume values and 95% confidence intervals derived from NSGA-II and MOEA/D are shown in Fig. 13. As with the results obtained from the previous example, the hypervolume outputs in Example II also indicate that NSGA-II performs better than MOEA/D in terms of solution diversity and convergence. In this example, the 95% confidence interval for the mean hypervolume based on 30 runs of NSGA-II is (0.3970, 0.3982), whereas that of MOEA/D is (0.3444, 0.3476). The analysis in the remainder of this section will be based on the top-performing run of NSGA-II which gives the largest hypervolume of 0.4007.

Fig. 14 illustrates the set of non-dominated solutions generated by the selected NSGA-II run. Note that these validated solutions are normalised for visualisation purposes. The plot indicates that it is an exacting task for a DM to comprehend all 726 solutions on the Pareto front and make a well-informed decision. Thus, a pruning operation will be performed in Step 3 to identify a manageable subset of solutions that strongly represent the original Pareto front.

7.2.3. Reduction of Pareto optimal solutions

We determine the relative diversity of representative solutions with K varied between 2 and 30. Fig. 15 shows a notable difference between the performance of the K-means and K-medoids methods. While the *REI* values of the K-means method improve gradually as K increases, the *RCI* values do not increase monotonically. Likewise, the *RCI* values of the K-medoids method increase steadily as more solutions are included in the representative set, whereas the *REI* values seem to improve until $K = 12$ after which point the *REI* values begin to fluctuate around the same level.

These results allow us to put forward the suggestion to use K-means over K-medoids in this example because the former tends to produce more reliable relative diversity results than the latter. As with the analysis shown in Example I, a DM can also make a direct trade-off between the interpretability and the relative diversity of the representative solutions from the plot in Fig. 15. For demonstration purposes, a representative set of 12 solutions, which is considered an elbow point in this case, is employed. The summary of the clustering results is exhibited in Appendix D.

7.3. Example III

The overall objectives of this example are to ensure the correctness and to understand the properties of the proposed pruning methods and relative diversity indicators. The analysis will be based on the well-known scalable multi-objective test problem

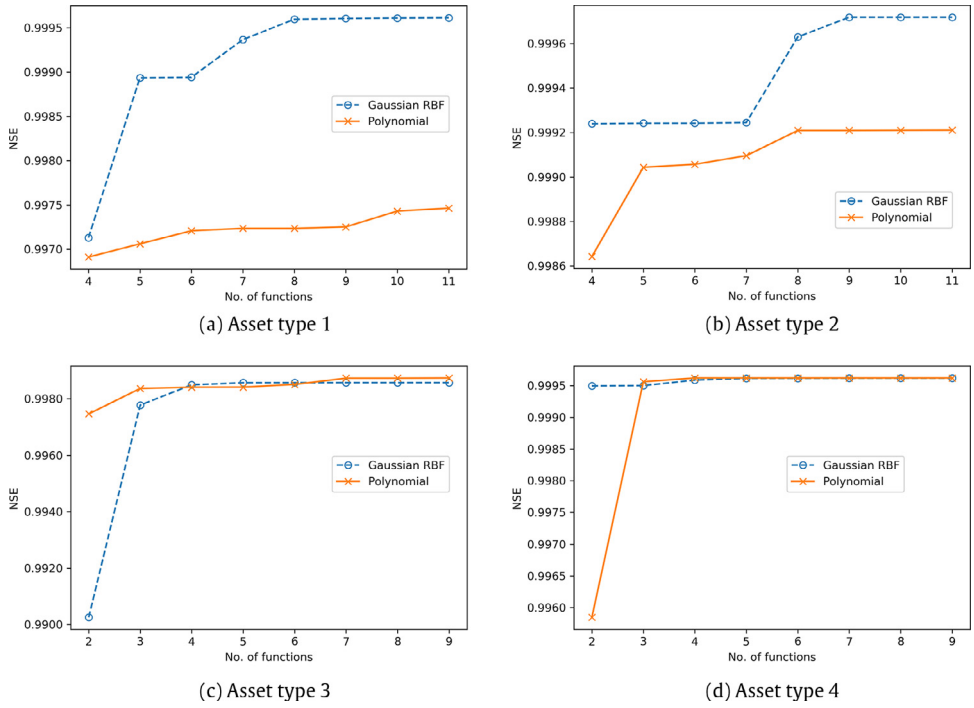

Fig. 11. Performance of approximation functions (Example II).

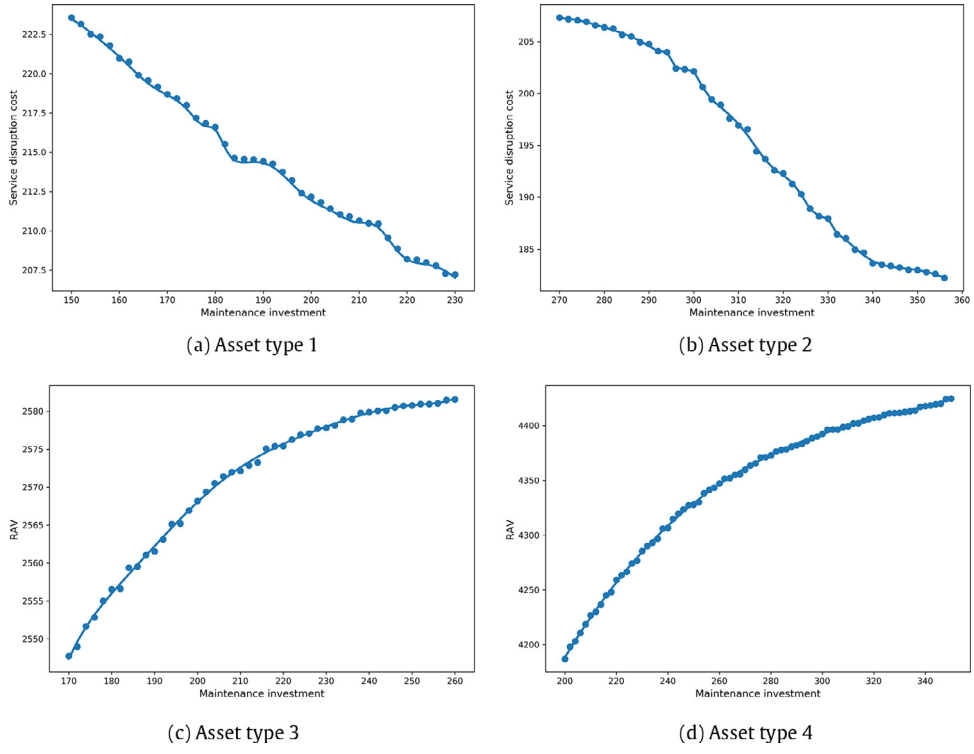

Fig. 12. Curve fitting for investment-performance relationships (Example II).

DTLZ2. The bi-objective version of DTLZ2 is chosen because of its ability to control shape and distribution of Pareto front.

In this example, the relative diversity indicators are tested against four different scenarios. The descriptions of these scenarios are given in Table 4. Scenario 1 is the case in which all representative solutions are bunched together around the centre of the Pareto front. This is a usual instance when a DM adopts an efficiency-based method to identify knee solutions. Representative solutions in Scenario 2 are the combination solutions that maximise the hypervolume value. Due to the problem's simplicity, solutions in Scenario 2 can be determined by a generic grid search method. We also follow the guidelines given in Eq. (14) for the reference point selection. The representative solutions given in Scenario 3 are the solutions that are closest to the centroids of clusters produced by the *K*-means method, whereas those shown in Scenario 4 are the medoids of the clusters generated by the *K*-medoids method.

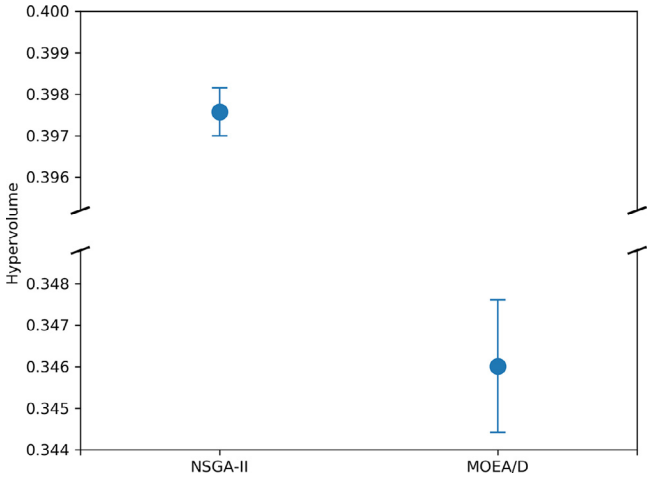

Fig. 13. 95% Confidence intervals for the mean hypervolume (Example II).

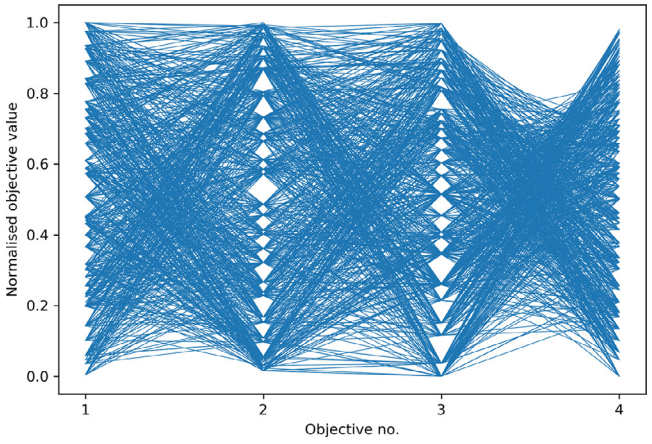

Fig. 14. Pareto set of validated solutions in the normalised scale (Example II).

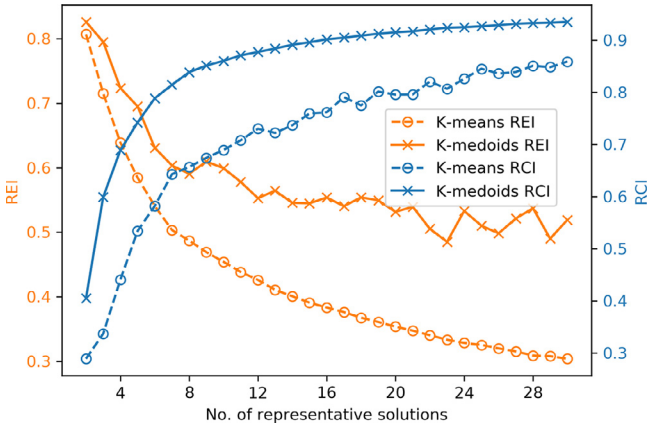

Fig. 15. Relative diversity against the number of representative solutions (Example II).

Table 4
Description of verification scenarios (Example III).

Scenario	Description
1	Representative solutions are bunched together around the centre of the Pareto front
2	Representative solutions are chosen to maximise hypervolume value
3	Representative solutions are shifted centroids of clusters produced by the *K*-means method
4	Representative solutions are medoids of clusters produced by the *K*-medoids method

Table 5
Relative diversity and hypervolume values of verification scenarios (Example III).

Scenario	REI	RCI	Hypervolume
Scenario 1	0.8950	0.1447	0.2059
Scenario 2	0.4114	0.8306	0.4378
Scenario 3	0.2864	0.9163	0.3668
Scenario 4	0.2901	0.9167	0.3755

For the sake of simplicity, we consider selecting four representative solutions from the Pareto front of 50 solutions in this example. The representative solutions for all verification scenarios are shown in Fig. 16, with the solution clusters differentiated by colours. The relative diversity and hypervolume results of all four scenarios are given in Table 5. Note that the clusters for Scenarios 1 and 2 are determined by the shortest Euclidean distance between the original and the representative solutions.

The results are in line with the general intuition that Scenario 1 produces the worst outputs among the four verification scenarios for all three indicators. Since all the solutions are only clustered around the centre of the frontier, one can expect that the solution diversity of this scenario is poor. Scenario 2, albeit maximising the hypervolume value by featuring the boundary solutions, does not produce satisfactory *REI* and *RCI* values. This is mainly because the incorporation of the boundary solutions forces that they locate further to intermediate representative solutions when compared to Scenarios 3 and 4. This instance, therefore, makes the clusters of intermediate solutions contain significantly larger number of solution members than those of boundary solutions do.

The results also indicate that the representative solutions in Scenarios 3 and 4 are distinctly superior to those in the first two scenario in terms of relative diversity. The two pruning methods give similar results, with *REI* indicating that the *K*-means method slightly outperforms the *K*-medoids method and *RCI* showing the opposite. This slight difference between the results produced by the two methods is due to the use of different topological measures. Specifically, since the angles between the solutions are employed, slightly extreme solutions are chosen in Scenario 3 as compared to Scenario 4 in which the solutions are selected according to the Euclidean distance. It is also important to mention that the numbers of solution members in clusters shown in Scenarios 3 and 4 are more evenly distributed than those in Scenario 2.

7.4. Discussion

The proposed data-driven approach was able to attain all the research goals set out in the problem description. Specifically, the approach demonstrated its capability to aggregate incommensurable inputs from different asset types, optimise investment decisions, and reduce the solutions on the Pareto front in the sense that it could preserve the relative diversity of the representative solutions as compared to the entire non-dominated solutions. All the steps could be executed in the absence of the DM' s preference. Furthermore, our analysis showed that the proposed performance indicators enabled the user to quantify the relative diversity of the representative solutions for problems in different dimensions. According to the results obtained from three numerical examples, we can make the following observations:

- *Investment-performance approximation functions:* In Examples I and II, it was apparent that we only chose the approximation functions that produce very effective *NSE* results ($NSE > 0.99$). The log-transformed and polynomial functions were shown to have a very limited application, as they could only capture the concave investment-performance relationships. On the other hand, the Gaussian RBFs, due to their flexibility, were able to

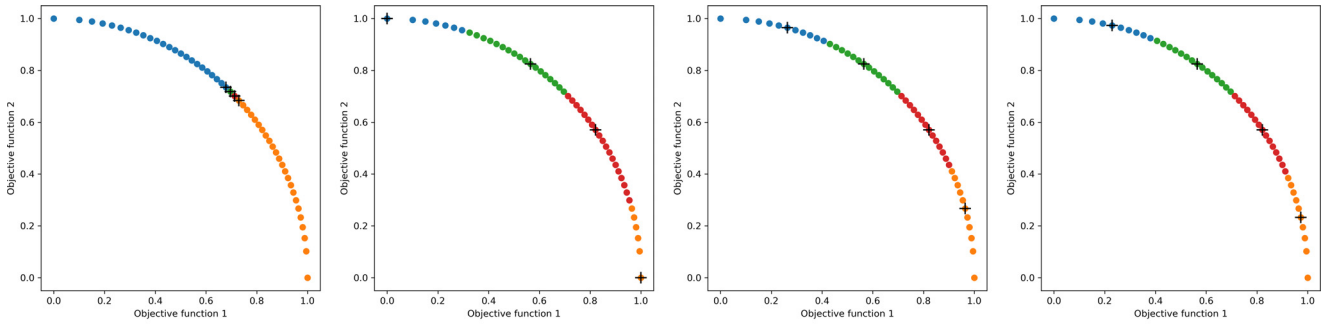

Fig. 16. Representative solutions and clusters of four verification scenarios (Example III).

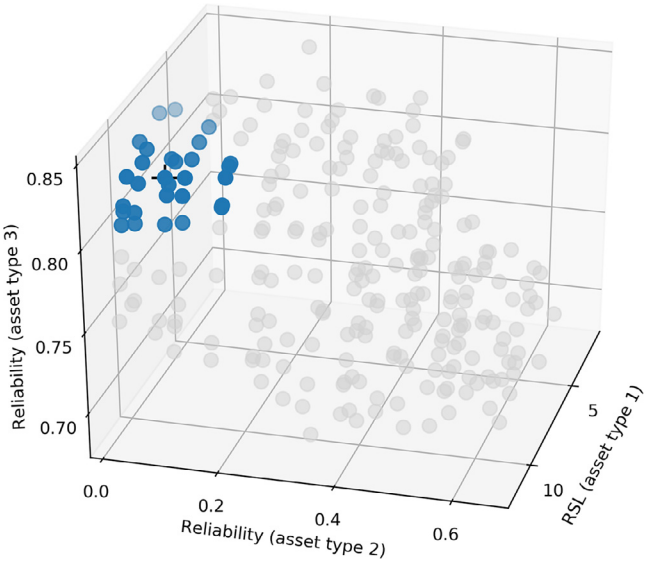

Fig. 17. Chosen representative solution and corresponding cluster (Example I).

produce very effective approximation functions in a wide range of data sets even though the data seemed to form a non-concave frontier with multiple inflection points. According to the numerical analyses, we can put forward a recommendation to use the Gaussian RBFs to approximate inputs for the portfolio optimisation model. Despite incurring high computational cost as compared to the log-transformed and polynomial functions, the Guassian RBFs can guarantee their convergence for different data characteristics. Moreover, due to the generalisability of these techniques, there is no restriction on the source of the performance measure. Our proposed method is applicable to the data obtained from any source such as an optimisation model, a simulation model, a computer experiment, and performance observations in a factory. An exception can be made for the data set with a distinctly concave relationship where the log-transformed and polynomial functions are more efficient.

- *Multi-objective optimisation:* In our particular examples in two- and three-dimensional space, NSGA-II was shown to outperform MOEA/D as the former produced more diverse solutions than the latter did according to the hypervolume indicator. Since the development of a problem-specific optimisation algorithm is not a major contribution of this work, we only demonstrated the applicability of our overall approach to different evolutionary algorithms. In other words, our approach relaxes the requirement on the use of original objective functions employed in the asset-type models, which generally incur high computational cost as evidenced in previous studies. More specifically, by using the approximation functions to simplify inputs and applying solution adjustment and validation operations after the optimisation stage, we showed that any existing or future MOEAs that can address constrained multi-objective problems with continuous variables and functions can be adopted to address this portfolio management problem.
- *Pruning methods:* The results obtained from all three examples indicated that both the *K*-means and *K*-medoids methods were effective in identifying representative solutions from a large set of optimal solutions according to a diversity criterion. The overall performance of both methods was closely comparable as they could identify diverse solution sets in two- and three-objective problems. The only slight difference in Example I was due to the marginal error arising from the shifted centroids in the *K*-means method. In Example III, the two pruning methods were also shown to identify more strongly representative solution of the entire Pareto front than those selected by a hypervolume maximising technique. Since the boundary solution in each objective is always chosen to maximise the hypervolume, this technique inevitably makes the clusters of intermediate solutions contain a large number of solution members. This means that the numbers of solution members in different clusters are less evenly distributed. Nonetheless, the difference between the *K*-means and *K*-medoids methods became more significant in the four-dimensional problem (Example II). The results indicated that the *K*-medoids method, albeit maximising the cosine similarity between the representative and other non-dominated solutions, performed poorly when considering the Euclidean indicator. This is because the convergence of the *K*-medoids method is more difficult to be achieved than that of the *K*-means method. Specifically, using the same number of maximum iterations for both methods in our experiments, the approximation process of medoids is shown to be less efficient than that of centroids. While the approximate medoids result from the assignment of completely different solutions in every iteration, the approximate centroids are slightly shifted throughout the iterations. According to these findings, we can put forward a suggestion to adopt the *K*-means method due to its consistency in problems with different dimensions. As an alternative, the DM can also employ the hypervolume maximising technique if he/she would like to incorporate very extreme solutions in the representative solution set.
- *Number of representative solutions:* From the sensitivity analyses in Examples I and II, both *REI* and *RCI* demonstrated that, at small *K* values, the relative diversity of representative solutions improved substantially as *K* increases. Nevertheless, the improvement became less significant once *K* reaches a certain

level. These results were in line with the general intuition that the improvement should be less significant when the majority of the area on the Pareto front is already covered by the representative solutions. To maintain the interpretability and diversity of the representative solutions, we suggest that the DM chooses the number of solutions at the elbow point of the sensitivity graph where the improvement in relative diversity begins to stall. An exception can be made in accordance with the DM's preferences.

- *Performance indicators for representative solutions:* All the numerical examples demonstrated the effectiveness of the proposed performance indicators, namely that both *REI* and *RCI* were able to quantify the relative diversity of the representative solutions as compared to the original solutions on the Pareto front. Apart from producing sensible results in the verification scenarios in Example III, both indicators also yielded nearly the same results in the sensitivity analysis of Example I. A plausible reason that the two indicators are closely comparable in the two- and three-dimensional problems is because all the solutions on the Pareto front are pushed to their limits in each of the objectives. Hence, the magnitude of all solution vectors is approximately the same, thereby alleviating the difference between the two topological indicators. The numerical experiments performed in Example III indicated that *RCI* gave more priority to slightly more extreme solutions on the Pareto front. Since the calculation of *RCI* is based on the angle between the solution vectors, the indicator is more sensitive to extreme solutions in order to preserve the average similarity between the selected and non-selected solutions. In essence, we suggest that, although the two measures are closely comparable, the DM relies on *RCI* if he/she wants to include slightly more extreme solutions in the representative set and employs *REI* if he/she prefers slightly more intermediate solutions and evenly distributed clusters.

After taking the three-step approach, the DM is faced with a set of representative solutions that strongly reflect the characteristics of original Pareto front. The proposed approach is expected to create a better understanding of the Pareto front and enable the DM to identify a region of his/her interest through choosing a preferred solution from the representative solution set. To demonstrate the post-pruning process, we revisit the non-dominated solutions and their corresponding representative solutions produced in Example I. In this demonstration, we assume that the DM is interested in and chooses an extreme solution as highlighted in Fig. 17. It is apparent that the chosen solution is basically the representative solution of a cluster that consists of 29 solution members. Hence, we suggest that the DM further investigates the selected cluster to identify the definitive solution. In general, we can offer two streams of recommendations for post-pruning steps:

- *Preference-based selection:* In case the selected cluster does not contain too many solutions, the DM can either choose a preferred solution directly from the cluster or employ MCDA methods to compare the solutions within the cluster. Conducive MCDA methods to this particular application include traditional pair-wise comparison and analytic hierarchy process (AHP), as they enable the DM to systematically prioritise the solutions (Watrobski et al., 2019).
- *Efficiency-based selection:* If there are still too many solutions in the selected cluster or it is still difficult to elicit the DM's preferences, we suggest that the DM applies an efficiency-based method. The application of efficiency-based methods such as a knee-based approach (Sudeng & Wattanapongsakorn, 2016) and data envelopment analysis (Li et al., 2009) after Pareto pruning can ensure the most efficient solution located within the region that is of interest to the DM.

8. Conclusions

In this paper, we proposed a three-step method for optimising and pruning budget allocation decisions for a portfolio management problem. The problem is inherently multi-objective, because a portfolio is comprised of assets from multiple categories of which performance metrics are not directly comparable. To address this problem, we employed a pruning method to reduce the number of Pareto optimal solutions. The ultimate goal of this paper was to deliver a small yet diverse set of solutions to the DM. Since the proposed approach is independent of user preferences, its outputs can be very informative for a DM who has limited knowledge of the problem domain.

In the first step, the relationship between the investment and performance of each asset type was determined. It was evident that the Gaussian RBFs were highly flexible and well capable of approximating functions for complex relationships when compared to the log-transformed power and polynomial functions. The chosen simplified functions led to efficient optimisation in the second step. The two widely-used MOEAs, NSGA-II and MOEA/D, were implemented. After the solutions were generated, adjusted, and validated, the hypervolume metrics revealed that NSGA-II was superior to MOEA/D in terms of solution convergence and diversity. In the final step, we employed the *K*-means and *K*-medoids clustering methods to prune the Pareto optimal solutions. Our experiments that benchmarked the two pruning methods against the hypervolume-maximising method demonstrated that the pruning methods were able to identify better representative solutions of the Pareto front with more evenly distributed clusters. To measure the spread of representative solutions over the Pareto front, we developed two relative diversity indicators based on Euclidean distance and cosine similarity metrics. These metrics are easily comprehensible as they are scaled with respect to extreme reference scenarios. We demonstrated through numerical examples that budget allocation decisions could be efficiently optimised and that the number of Pareto optimal solutions could be greatly reduced. Corroborated by both the indicators and the solution visualisation, the proposed approach was found to maintain high integrity of the original Pareto front. We also put forward suggestions on further steps towards obtaining the final solution and guidelines on choosing appropriate pruning methods and indicators.

We can offer four streams of recommendations for future research. Firstly, in this paper, we assumed that the outputs obtained from the asset-type models are perfectly accurate and deterministic. If the information about risks associated with investment choices and system performance can be acquired, it will open up an opportunity to develop a stochastic portfolio optimisation model. Moreover, there is also an avenue for integrating our proposed performance indicators with the Pareto Uncertainty Index (Selcuklu, Coit, & Felder, 2020) to address representative solutions in a stochastic setting. Secondly, the proposed approach works on the assumption that the number of assets is known and fixed for each asset type. This assumption limits the decisions that can be made in the proposed optimisation model. Hence, we suggest that future studies could relax this assumption so that not only intervention options but also system enhancement plans (e.g. additional asset acquisition) can also be decided by the model. Thirdly, the approximation function proposed in this paper is only applicable to a two-dimensional relationship, namely one investment variable and one performance variable in our specific problem. To enhance the practicality of the model, more performance objectives should be incorporated in the model. Hence, it is suggested that future research delve into the application of a symbolic regression method based on genetic programming (Ghaddar, Sakr, & Asiedu, 2016) in the approximation of investment-performance relationships in high-dimensional space.

Fourthly, the problem of our interest also opens up a research avenue in the development of a problem-specific optimisation algorithm. Application of algorithms that are capable of making a solution reparation during the optimisation such as Darwinian (Nowak & Sigmund, 2004) or Lamarckian (Ong & Keane, 2004) algorithms could be the key to a more efficient approach.

Acknowledgments

The authors would like to thank three anonymous reviewers for their constructive comments that significantly improve the quality of this paper. The authors are thankful to Dr Kamran Moghaddam, Dr Qiang Bai, and Dr Shuya Zhong for the data employed in the case example. The authors would also like to thank Network Rail Limited for their support in carrying out this work. This work was also supported by the Engineering and Physical Sciences Research Council (EPSRC) through the BT Prosperity Partnership Project: Next Generation Converged Digital Infrastructure under Grant EP/R004935/1. The first author wishes to acknowledge the support provided by the Department of Mathematics, Mahidol University.

Supplementary material

Supplementary material associated with this article can be found, in the online version, at 10.1016/j.ejor.2021.04.053.

References

Araya, I., Moyano, M., & Sanchez, C. (2020). A beam search algorithm for the biobjective container loading problem. *European Journal of Operational Research, 286*(2), 417–431. https://doi.org/10.1016/j.ejor.2020.03.040.

Bai, Q., Ahmed, A., Li, Z., & Labi, S. (2015). A hybrid Pareto frontier generation method for trade-off analysis in transportation asset management. *Computer-Aided Civil and Infrastructure Engineering, 30*(3), 163–180. https://doi.org/10.1111/mice.12079.

Brusco, M. J. (2017). Partitioning methods for pruning the Pareto set with application to multiobjective allocation of a cross-trained workforce. *Computers & Industrial Engineering, 111*, 29–38. https://doi.org/10.1016/j.cie.2017.06.035.

Cao, R., Hou, W., & Gao, Y. (2018). An entropy-based three-stage approach for multi-objective system reliability optimization considering uncertainty. *Engineering Optimization, 50*(9), 1453–1469. https://doi.org/10.1080/0305215X.2017.1402014.

Chattopadhyay, K. D., Verma, S., Satsangi, P. S., & Sharma, P. C. (2009). Development of empirical model for different process parameters during rotary electrical discharge machining of copper-steel (EN-8) system. *Journal of Materials Processing Technology, 209*(3), 1454–1465. https://doi.org/10.1016/j.jmatprotec.2008.03.068.

Chettibi, T. (2019). Smooth point-to-point trajectory planning for robot manipulators by using radial basis functions. *Robotica, 37*(3), 539–559. https://doi.org/10.1017/S0263574718001169.

De Santiago-Perez, J. J., Osornio-Rios, R. A., Romero-Troncoso, R. J., & Morales-Velazquez, L. (2013). FPGA-based hardware CNC interpolator of Bezier, splines, B-splines and NURBS curves for industrial applications. *Computers & Industrial Engineering, 66*(4), 925–932. https://doi.org/10.1016/j.cie.2013.08.024.

Deb, K., Agrawal, S., Pratap, A., & Meyarivan, T. (2000). A fast elitist non-dominated sorting genetic algorithm for multi-objective optimization: NSGA-II. *Lecture Notes in Computer Science, 1917*, 849–858.

France-Mensah, J., O'Brien, W. J., & Khwaja, N. (2019). Impact of multiple highway funding categories and project eligibility restrictions on pavement performance. *Journal of Infrastructure Systems, 25*(1). https://doi.org/10.1061/(ASCE).

Fwa, T. F., & Farhan, J. (2012). Optimal multiasset maintenance budget allocation in highway asset management. *Journal of Transportation Engineering, 138*(10), 1179–1187. https://doi.org/10.1061/(ASCE)TE.1943-5436.0000414.

Ghaddar, B., Sakr, N., & Asiedu, Y. (2016). Spare parts stocking analysis using genetic programming. *European Journal of Operational Research, 252*(1), 136–144. https://doi.org/10.1016/j.ejor.2015.12.041.

Gneiting, T. (2013). Strictly and non-strictly positive definite functions on spheres. *Bernoulli, 19*(4), 1327–1349. https://doi.org/10.3150/12-BEJSP06.

Gong, C., & Zhou, W. (2018). Multi-objective maintenance strategy for in-service corroding pipelines using genetic algorithms. *Structure and Infrastructure Engineering, 14*(11), 1561–1571. https://doi.org/10.1080/15732479.2018.1459744.

Guo, Z. X., Wong, W. K., Li, Z., & Ren, P. (2013). Modeling and Pareto optimization of multi-objective order scheduling problems in production planning. *Computers & Industrial Engineering, 64*(4), 972–986. https://doi.org/10.1016/j.cie.2013.01.006.

Habermann, C., & Kindermann, F. (2007). Multidimensional spline interpolation: Theory and applications. *Computational Economics, 30*(2), 153–169. https://doi.org/10.1007/s10614-007-9092-4.

Hafiz, F., Swain, A., & Mendes, E. (2020). Multi-objective evolutionary framework for non-linear system identification: A comprehensive investigation. *Neurocomputing, 386*, 257–280. https://doi.org/10.1016/j.neucom.2019.12.095.

Hartikainen, M., Miettinen, K., & Klamroth, K. (2019). Interactive nonconvex Pareto Navigator for multiobjective optimization. *European Journal of Operational Research, 275*(1), 238–251. https://doi.org/10.1016/j.ejor.2018.11.038.

Ishibuchi, H., Imada, R., Setoguchi, Y., & Nojima, Y. (2018). How to specify a reference point in hypervolume calculation for fair performance comparison. *Evolutionary Computation, 26*(3), 411–440. https://doi.org/10.1162/EVCO_a_00226.

Kaufmann, L., & Rousseeuw, P. (1987). Clustering by means of medoids. *Data Analysis based on the L1-Norm and Related Methods*, 405–416.

Kellner, F., Lienland, B., & Utz, S. (2019). An a posteriori decision support methodology for solving the multi-criteria supplier selection problem. *European Journal of Operational Research, 272*(2), 505–522. https://doi.org/10.1016/j.ejor.2018.06.044.

Kingma, D. P., & Ba, J. (2014). Adam: A method for stochastic optimization. arXiv preprint arXiv:1412.6980,.

Koumousis, V. K., & Katsaras, C. P. (2006). A saw-tooth genetic algorithm combining the effects of variable population size and reinitialization to enhance performance. *IEEE Transactions on Evolutionary Computation, 10*(1), 19–28. https://doi.org/10.1109/TEVC.2005.860765.

Kulturel-Konak, S., Coit, D. W., & Baheranwala, F. (2008). Pruned Pareto-optimal sets for the system redundancy allocation problem based on multiple prioritized objectives. *Journal of Heuristics, 14*(4), 335–357. https://doi.org/10.1007/s10732-007-9041-3.

Li, Z., Liao, H., & Coit, D. W. (2009). A two-stage approach for multi-objective decision making with applications to system reliability optimization. *Reliability Engineering and System Safety, 94*(10), 1585–1592. https://doi.org/10.1016/j.ress.2009.02.022.

Ma, T., Liu, Y., & Cao, C. (2019). Neural networks for 3D temperature field reconstruction via acoustic signals. *Mechanical Systems and Signal Processing, 126*, 392–406. https://doi.org/10.1016/j.ymssp.2019.02.037.

MacQueen, J. (1967). Some methods for classification and analysis of multivariate observations. In *Proceedings of the fifth Berkeley symposium on mathematical statistics and probability: vol. 1* (pp. 281–297). Oakland, CA, USA.

Moghaddam, K. S. (2013). Multi-objective preventive maintenance and replacement scheduling in a manufacturing system using goal programming. *International Journal of Production Economics, 146*(2), 704–716. https://doi.org/10.1016/j.ijpe.2013.08.027.

Nash, J. E., & Sutcliffe, J. V. (1970). River flow forecasting through conceptual models part i a discussion of principles. *Journal of Hydrology, 10*(3), 282–290. https://doi.org/10.1016/0022-1694(70)90255-6.

Nicolai, R. P., & Dekker, R. (2008). Optimal maintenance of multi-component systems: A review. *Springer Series in Reliability Engineering, 8*, 263–286. https://doi.org/10.1007/978-1-84800-011-7_11.

Nowak, M. A., & Sigmund, K. (2004). Evolutionary dynamics of biological games. *Science, 303*(5659), 793–799. https://doi.org/10.1126/science.1093411.

Olde Keizer, M. C. A., Flapper, S. D. P., & Teunter, R. H. (2017). Condition-based maintenance policies for systems with multiple dependent components: A review. *European Journal of Operational Research, 261*(2), 405–420.

Ong, Y. S., & Keane, A. J. (2004). Meta-Lamarckian learning in memetic algorithms. *IEEE Transactions on Evolutionary Computation, 8*(2), 99–110. https://doi.org/10.1109/TEVC.2003.819944.

Pang, L. M., Ishibuchi, H., & Shang, K. (2019). Offline automatic parameter tuning of MOEA/d using genetic algorithm. In *Proceedings of the IEEE symposium series on computational intelligence (SSCI)* (pp. 1889–1897).

Petchrompo, S., Li, H., Erguido, A., Riches, C., & Parlikad, A. K. (2020). A value-based approach to optimising long-term maintenance plans for a multi-asset k-out-of-N system. *Reliability Engineering & System Safety*, 106924. https://doi.org/10.1016/j.ress.2020.106924.

Petchrompo, S., & Parlikad, A. K. (2019). A review of asset management literature on multi-asset systems. *Reliability Engineering & System Safety, 181*, 181–201. https://doi.org/10.1016/j.ress.2018.09.009.

Raimundo, M. M., Ferreira, P. A. V., & Von Zuben, F. J. (2020). An extension of the non-inferior set estimation algorithm for many objectives. *European Journal of Operational Research, 284*(1), 53–66. https://doi.org/10.1016/j.ejor.2019.11.017.

Rasmekomen, N., & Parlikad, A. K. (2013). Maintenance optimization for asset systems with dependent performance degradation. *IEEE Transactions on Reliability, 62*(2), 362–367. https://doi.org/10.1109/TR.2013.2257056.

Sacco, T., Compare, M., Zio, E., & Sansavini, G. (2019). Portfolio decision analysis for risk-based maintenance of gas networks. *Journal of Loss Prevention in the Process Industries, 60*, 269–281. https://doi.org/10.1016/j.jlp.2019.04.002.

Sahoo, L., Bhunia, A. K., & Kapur, P. K. (2012). Genetic algorithm based multi-objective reliability optimization in interval environment. *Computers & Industrial Engineering, 62*(1), 152–160. https://doi.org/10.1016/j.cie.2011.09.003.

Samsuri, S. F. M., Ahmad, R., Zakaria, M. Z., & Zain, M. Z. M. (2019). Parameter tuning for comparing multi-objective evolutionary algorithms applied to system identification problems. In *Proceedings of the IEEE international conference on smart instrumentation, measurement and application (ICSIMA)* (pp. 1–6).

Selcuklu, S. B., Coit, D. W., & Felder, F. A. (2020). Pareto uncertainty index for evaluating and comparing solutions for stochastic multiple objective problems. *European Journal of Operational Research, 284*(2), 644–659. https://doi.org/10.1016/j.ejor.2020.01.004.

Serfidan, A. C., Uzman, F., & Turkay, M. (2020). Optimal estimation of physical properties of the products of an atmospheric distillation column using support vector regression. *Computers & Chemical Engineering, 134*. https://doi.org/10.1016/j.compchemeng.2019.106711.

Sideratos, G., & Hatziargyriou, N. D. (2020). A distributed memory RBF-based model for variable generation forecasting. *International Journal of Electrical Power and Energy Systems, 120*. https://doi.org/10.1016/j.ijepes.2020.106041.

Sudeng, S., & Wattanapongsakorn, N. (2015). Post Pareto-optimal pruning algorithm for multiple objective optimization using specific extended angle dominance. *Engineering Applications of Artificial Intelligence, 38*, 221–236. https://doi.org/10.1016/j.engappai.2014.10.020.

Sudeng, S., & Wattanapongsakorn, N. (2016). A knee-based multi-objective evolutionary algorithm: an extension to network system optimization design problem. *Cluster Computing, 19*(1), 411–425. https://doi.org/10.1007/s10586-015-0492-2.

Taboada, H., & Coit, D. (2007). Data clustering of solutions for multiple objective system reliability optimization problems. *Quality Technology & Quantitative Management, 4*(2), 191–210. https://doi.org/10.1080/16843703.2007.11673145.

Taboada, H. A., Baheranwala, F., Coit, D. W., & Wattanapongsakorn, N. (2007). Practical solutions for multi-objective optimization: An application to system reliability design problems. *Reliability Engineering and System Safety, 92*(3), 314–322. https://doi.org/10.1016/j.ress.2006.04.014.

Taboada, H. A., & Coit, D. W. (2008). Multi-objective scheduling problems: Determination of pruned Pareto sets. *IIE Transactions (Institute of Industrial Engineers), 40*(5), 552–564. https://doi.org/10.1080/07408170701781951.

Ustun, A. K., & Anagun, A. S. (2015). Multi-objective mitigation budget allocation problem and solution approaches: The case of istanbul. *Computers & Industrial Engineering, 81*, 118–129. https://doi.org/10.1016/j.cie.2014.12.025.

Wang, W., Li, K., Tao, X., & Gu, F. (2020a). An improved MOEA/D algorithm with an adaptive evolutionary strategy. *Information Sciences, 539*, 1–15. https://doi.org/10.1016/j.ins.2020.05.082.

Wang, W., Lin, M., Fu, Y., Luo, X., & Chen, H. (2020b). Multi-objective optimization of reliability-redundancy allocation problem for multi-type production systems considering redundancy strategies. *Reliability Engineering & System Safety, 193*. https://doi.org/10.1016/j.ress.2019.106681.

Watrobski, J., Jankowski, J., Ziemba, P., Karczmarczyk, A., & Ziolo, M. (2019). Generalised framework for multi-criteria method selection. *Omega (United Kingdom), 86*, 107–124. https://doi.org/10.1016/j.omega.2018.07.004.

Yang, T., Gao, X., Sellars, S. L., & Sorooshian, S. (2015). Improving the multi-objective evolutionary optimization algorithm for hydropower reservoir operations in the California oroville-thermalito complex. *Environmental Modelling and Software, 69*, 262–279. https://doi.org/10.1016/j.envsoft.2014.11.016.

Zhang, Q., & Li, H. (2007). MOEA/D: A multiobjective evolutionary algorithm based on decomposition. *IEEE Transactions on Evolutionary Computation, 11*(6), 712–731.

Zhong, S., Pantelous, A. A., Beer, M., & Zhou, J. (2018). Constrained non-linear multi-objective optimisation of preventive maintenance scheduling for offshore wind farms. *Mechanical Systems and Signal Processing, 104*, 347–369. https://doi.org/10.1016/j.ymssp.2017.10.035.

Zio, E., & Bazzo, R. (2011). A clustering procedure for reducing the number of representative solutions in the Pareto Front of multiobjective optimization problems. *European Journal of Operational Research, 210*(3), 624–634. https://doi.org/10.1016/j.ejor.2010.10.021.

Zitzler, E., & Thiele, L. (1999). Multiobjective evolutionary algorithms: A comparative case study and the strength Pareto approach. *IEEE Transactions on Evolutionary Computation, 3*(4), 257–271. https://doi.org/10.1109/4235.797969.